Ore Geology Reviews 143 (2022) 104722

Contents lists available at ScienceDirect

Ore Geology Reviews

journal homepage: www.elsevier.com/locate/oregeorev

Review

Bismuth: Economic geology and value chains

Eimear Deady [a,c,*], Charlie Moon [b,c], Kathryn Moore [c], Kathryn M. Goodenough [a], Robin K. Shail [c]

[a] British Geological Survey, The Lyell Centre, Edinburgh EH14 4AP, United Kingdom
[b] Rose Cottage, Church Hill, Calstock, Cornwall PL18 9QQ, United Kingdom
[c] Camborne School of Mines, University of Exeter, Penryn Campus, Cornwall TR10 9FE, United Kingdom

ARTICLE INFO

Keywords:
Bismuth
Mineralisation
Critical metal
Collector element
Production
Geochemistry
Supply chain

ABSTRACT

Bismuth occurs in a wide range of mineral deposit types and is usually regarded as a deleterious by-product. Its classification as a critical raw material by the European Commission in 2017 and a critical mineral by the USA in 2018 has, however, reawakened interest in Bi production and its security of supply. Demand for Bi is increasing, mostly as a substitute for Pb and for use in chemicals. Bismuth is mainly chalcophile in behaviour, although it has some lithophile characteristics. The element is strongly concentrated in felsic crustal lithologies, particularly fractionated granites, where it can substitute for Zr in zircon. It occurs within a diverse range of minerals; the most important hydrothermal minerals are native bismuth and bismuthinite. Bismuth can substitute for Pb in galena and Bi-rich galena is a major Bi ore. Bismuth alloys with gold to form maldonite at temperatures $< 373\ ^{\circ}C$, thereby acting as a Au collector in felsic melts, particularly under reduced conditions. In the weathering environment Bi is generally immobile: it forms Bi oxide or hydroxide ochres or co-precipitates with Fe.

Bismuth is found in a range of mineralised systems, sometimes in sufficient quantities to be economically extracted as a by-product. The most common sources of Bi are W-, Pb-, and, occasionally, Au-rich skarns, while five element (Co-Ni-Bi-Ag-As ± U) vein deposits were historically a major source of native Bi. Bismuth also occurs in large magmatic systems such in Sn- and W-rich greisens and associated veins as native bismuth and bismuthinite. Bismuth is present in trace concentrations in porphyry-hosted Mo-W-mineralisation and in some reduced intrusion-related Au, as well as some orogenic Au, deposits. VMS deposits can host minor Bi mineralisation, typically associated with the Au-rich parts of the mineralised system.

Bismuth supply is strongly reliant on Asian production; notably the skarns deposits Núi Pháo in Vietnam and Shizhuyuan in China. Alternative supplies of Bi could be unlocked by greater consideration of bismuth by-production at the evaluation stage of polymetallic prospects elsewhere, and if more sustainable recovery techniques are developed for retrieval of Bi from conventional mineral processing circuits.

The knowledge base for bismuth can be improved upon through interventions at the exploration, resource and reserve reporting and mineral processing planning stages. This in turn would provide a greater understanding of the deportment of Bi-bearing minerals, impacting on the design of mineral processing flow sheets and reducing waste, and thereby improving the sustainability and environmental footprint of mineral deposits.

1. Introduction

Pure bismuth (Bi) is a white, brittle metal with a slight pink colour. It was discovered by an unknown alchemist around 1400 CE, but no reliable descriptions appeared in Europe until later in the 15th century. First mined in Schneeberg, Germany around 1460, it was used as a pigment in paint. It was first shown to be a distinct element in 1753 by Claude Geoffrey the Younger (Mohan, 2010).

Critical metals have significant economic importance and are at risk of supply interruption. Bismuth is economically important for the production of some pharmaceutical products and as a substitute for Pb in paint. It has been recognised as a critical raw material by the European Commission (2017a), European Commission (2020a), Australia (Commonwealth of Australia, 2020), the United States (U.S. Department of the Interior, 2018), and by the British Geological Survey (2011, 2012, 2015).

* Corresponding author at: British Geological Survey, The Lyell Centre, Edinburgh EH14 4AP, United Kingdom.
E-mail address: eimear@bgs.ac.uk (E. Deady).

https://doi.org/10.1016/j.oregeorev.2022.104722
Received 22 March 2021; Received in revised form 20 December 2021; Accepted 19 January 2022
Available online 29 January 2022

Global production of Bi is concentrated at the Núi Pháo mine in Vietnam and as a by-product of Pb and W mining in China. The EU is thus 100% reliant on imports of primary refined Bi metal with a purity of at least 99.8% (European Commission, 2017b; European Commission, 2020a). The United States has also been 100% reliant on imports of Bi since 1997, when the last primary Bi refinery closed (U.S. Geological Survey, 2021). An additional factor contributing to the classification of Bi as a critical metal is the low end-of-life recycling rate, approximately <1% (European Commission, 2017b; European Commission, 2020b).

This contribution provides an overview of the economic geology of bismuth. It summarises the behaviour of bismuth in the crust and mantle, and the mineralogy of bismuth minerals. It then focusses on the geochemical processes that control bismuth mineralisation and the types of mineral deposits that contain significant bismuth. This is followed by a discussion on the economics of the bismuth market, including production, resources and reserves, demand, uses, recycling, substitution and the outlook for bismuth.

2. Bismuth in the crust and mantle

Bismuth is a group V element and is predominantly metallic. It has a strong tendency to assume the Bi^{3+} state (Angino, 1979). It occurs in the trivalent form in crustal fluids and its coordination chemistry is influenced by the presence of a lone electron pair (Brugger et al., 2016). Bismuth is diamagnetic and has one of the lowest thermal conductivity values amongst metals (Mintser, 1979, Mohan, 2010). It is a chalcophile element, with a high sulphide-silicate melt partition coefficient ($D^{sulf/sil}$ = 316), and it is compatible in magmatic sulphides (Jenner, 2017). The affinity of Bi for crustal, rather than mantle lithologies is clear from the average upper continental crust concentration of 0.16 mg/kg (Rudnick and Gao, 2003), versus the average primitive mantle concentration of 0.0025 mg/kg (McDonough and Sun, 1995).

A significant proportion of the primary Bi content of the bulk oceanic crust, prior to hydrothermal alteration and sulphide precipitation, is hosted by volcanic glass in the upper oceanic crust (Jenner, 2017). Bismuth is released from the subducting slab into the mantle wedge above a subduction zone, as indicated by its enrichment in primitive back arc basin basalts relative to Mid Ocean Ridge Basalt (MORB) (Jenner, 2017). The implication is that the majority of Bi host-phases in the upper oceanic crust are unstable during subduction, permitting their mobilisation by slab-derived fluids. Where there is variation in Bi content of global subduction-zone magmas, this is likely due to overprinting by a sedimentary component in the melt (Jenner, 2017). Potential hosts of Bi include low-temperature hydrothermal sulphides, sulphosalts and serpentine minerals (Jenner, 2017).

Bismuth becomes enriched during fractional crystallisation and formation of granite (Jochum and Hofmann, 1997, Zierenberg et al., 1993) and calc-alkaline and tholeiitic magmatic suites (Greenland et al., 1973). Recent data from Simons et al. (2017) indicate that the enrichment in the Variscan Cornubian Batholith of south west England (mean 0.53 ppm Bi, possibly including a minor contribution from weakly mineralised samples) is correlated with B- and F-rich granites as proposed by Ball et al. (1982). The Bi enrichment correlates at least crudely with fractionation and the occurrence of vein Sn mineralisation in this major Sn province. An example of increased Bi content in a fractionated granite is at Timbarra (Australia), where Bi is enriched to 5–20 times its average crustal abundance (Mustard et al., 2006). Bi enrichment in the highly fractionated Variscan Podlesí granite (Czech Republic) is extreme relative to most granites and a variety of other lithologies (Table 1). Zircon at Podlesí has incorporated Bi (up to 9 wt%), facilitated by the coupled substitution of P and Bi for Si and Zr (Breiter et al., 2006).

Recent geochemical atlases provide considerable information on regional Bi distribution where an ICP-MS analytical technique has been used (e.g. De Caritat and Cooper, 2016, Knights, 2020). A good example is that of European agricultural soils (Reimann et al., 2014); the median concentration was 0.14 ppm Bi in A horizon soils using an aqua regia leach. Most anomalies (>0.5 ppm Bi) in this dataset spatially correlate with Variscan granitoids, alkaline rocks in southern Europe and major tectonic lineaments in the Alps.

Table 1
Typical Bi concentration in geological and waste materials. Representative concentrations are provided for representative rock samples, the range of concentrations, or as an average of number of analyses (n), as a function of reporting style where Bi is included in analyses.

Bi (ppm)	Lithology	Location	Reference
0.5–24	Oceanic manganese nodules	N/A	Carlin et al., 1985
≤30	Coal ash	N/A	Carlin et al., 1985
0.028–0.038	Dolerite	Great Lake, Tasmania, Australia	Greenland et al., 1973
0.034	Granophyre	Great Lake, Tasmania, Australia	Greenland et al., 1973
0.03	Gabbro	Southern California Batholith, USA	Greenland et al., 1973
0.023–0.056	Felsic igneous rocks	Southern California Batholith, USA	Greenland et al., 1973
0.058–0.151	Felsic igneous rocks	Idaho Batholith, USA	Greenland et al., 1973
0.53	Average granite (n = 89)	Cornubian Batholith, south west England, UK	Simons et al., 2017
2.4	Average leucogranite (n = 5)	Himalaya, Nepal; Tibet	Wu et al., 2020
560–720	Granite	Podlesí, Czech Republic	Breiter et al., 2006

3. Mineralogy

Christy (2015) defines the diversity index (D) of an element as the ratio of observed mineral species to those predicted from a trend, based on the crustal abundance of a chemical element and the number of mineral species in which that element is an essential constituent. Bismuth is an essential component in 206 mineral species and has a diversity index (D) value of 19, second only to Te (D value 22), which classifies it as extremely diverse. This mineralogical diversity is due to its distinctly chalcophile nature and its intermediate electronegativity values that allow Bi to bond to a wide range of ligands (Christy, 2015). Bismuth occurs as anions, cations and in its native elemental form (Christy, 2015). Synthetic Bi mineral specimens are widely available; these exhibit hopper-like (a terraced structure indenting towards the centre) structures in pseudocubic crystals (Fig. 1A).

The compositional and crystallographic properties of Bi minerals have been determined by many researchers including Ciobanu and Cook (2000), Pring and Etschmann (2002), Ciobanu and Cook (2004), Ciobanu et al. (2005), Ciobanu et al. (2006a), Ciobanu et al. (2006b), Cook et al. (2007a), Cook et al. (2007b), Ciobanu et al. (2009), Voronin and Osadchii (2013), Voudouris et al. (2013), Makovicky and Topa (2014), Buzatu et al. (2015) and Fuertes-Fuente et al. (2016).

Common Bi minerals occurring in hydrothermal and magmatic systems can be divided into four groups: native bismuth (Fig. 1B and C) and alloys with Au and Ag; sulphides (Fig. 1B) and sulphosalts such as bismuthinite (Bi_2S_3); oxides (Fig. 1D) and oxysalts (Ball et al., 1982) such as bismutite $(BiO)_2CO_3$; and selenides and tellurides (Table 2).

The most important primary ore is bismuthinite, but there is also significant production from Bi-bearing galena. Gold and Bi commonly exhibit similar paragenetic and spatial relations during ore formation (Ciobanu et al., 2010). Bismuth-sulphosalts are relatively common components of Au-Ag ore deposits where they display a close paragenetic association with native gold (Li et al., 2019 and references therein). Bi-sulphosalts can be hosts of minor Au in a range of ore systems (Ciobanu et al., 2009). Maldonite (Au_2Bi) is one of the key Bi minerals associated with Au deposits and the only known naturally

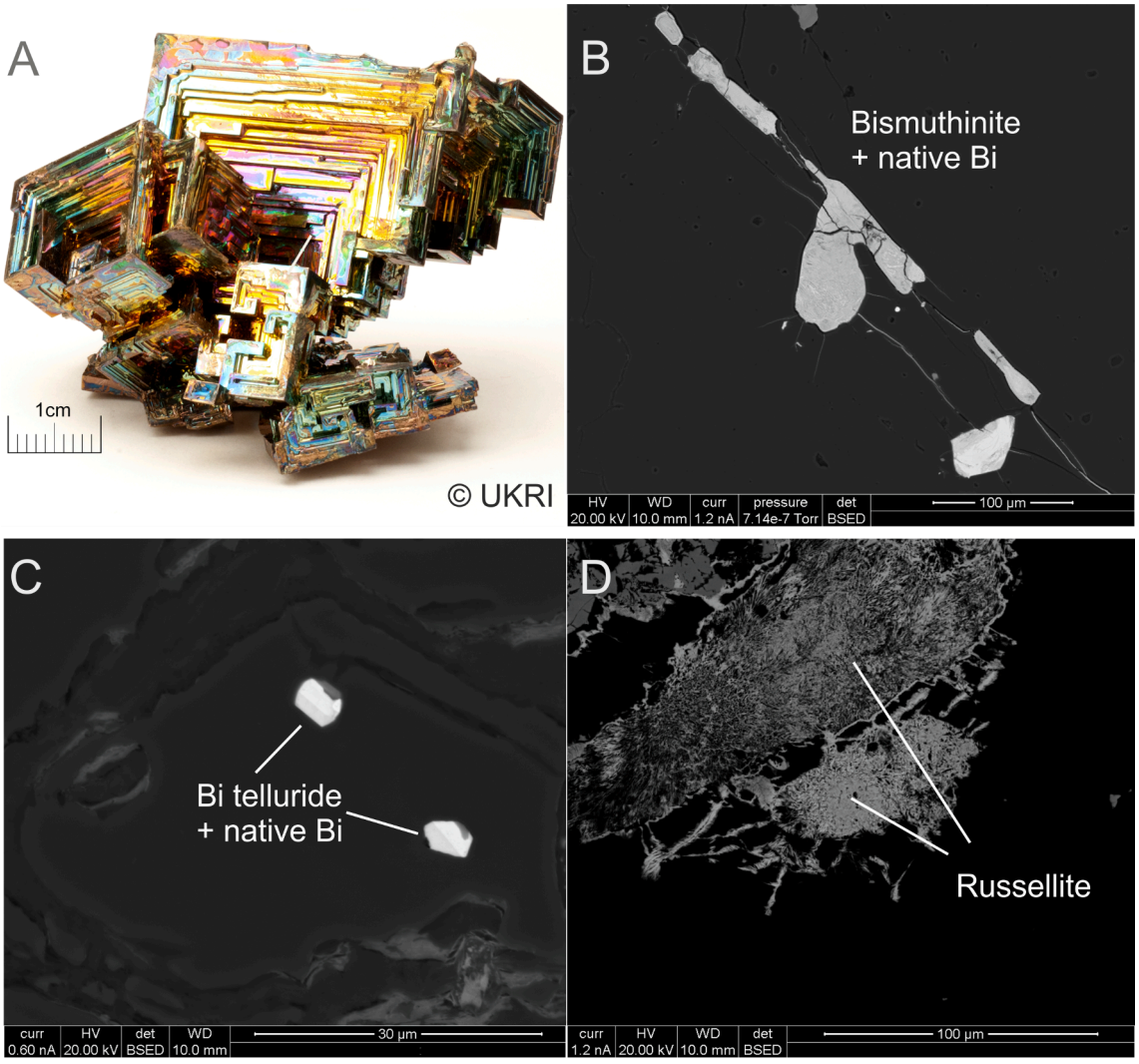

Fig. 1. Examples of the occurrence and habit of bismuth minerals. A. Synthetic bismuth hopper aggregate; B. Bismuthinite and blebby native bismuth along quartz grain boundaries from a granite-greisen vein (Bray Down, Cornwall); C. Euhedral to sub-euhedral bismuth melt inclusions with native bismuth, Bi-telluride, chalcopyrite and electrum in humite ($(Mg,Fe)_7(SiO_4)_3(F,OH)_2$) from a gold-bearing skarn in Mexico (reproduced with permission from Lacinska and Rochelle, 2019); D. Fibrous secondary russellite on wolframite in a wolframite-quartz vein from a granite-greisen vein (Hemerdon, Devon).

Table 2
Bismuth-bearing minerals.

Metallic bismuth and alloys with Au and Ag		Bismuth tellurides	
Native bismuth	Bi	Tsumoite	BiTe
Maldonite	Au_2Bi	Tellurobismuthite	Bi_2Te_3
Matildite	$AgBiS_2$	Pilsenite	Bi_4Te_3
Pavonite	$AgBi_3S_5$	Hedleyite	Bi_7Te_3
Jonassonite	$Au(Bi,Pb)_5S_4$	Tetradymite	Bi_2Te_2S
Bismuth sulphides and sulphosalts		Joésite -A	Bi_4TeS_2
Bismuthinite	Bi_2S_3	Joésite-B	Bi_4Te_2S
Ikunolite	Bi_4S_3	**Bismuth oxides and oxysalts**	
Emplectite	$CuBiS_2$	Bismite	Bi_2O_3
Junite	$(Bi_8Pb_3Cu_2(S,Se)_{16})$	Bismutite	$(BiO)_2CO_3$
Wittite	$(Pb_9Bi_{12}(S,Se)_{27})$	Bismoclite	BiOCl
Andorite	$PbAgSb_3S_6$	Russellite	Bi_2WO_6
Akinite	$PbCuBiS_3$	Montanite	$Bi_2TeO_6{\cdot}2H_2O$
Wittichenite	Cu_3BiS_3	Cannonite	$(Bi_2(SO_4)O(OH)_2)$
Galenobismutite	$PbBi_2S_4$	Preisingerite	$(Bi_3(AsO_4)_2O(OH))$
Cosalite	$Pb_2Bi_2S_5$	Bismutoferrite	$(Fe^{3+}{}_2Bi(SiO_4)_2(OH))$
Lillianite	$Pb_3Bi_2S_6$		

occurring compound of the two elements, named after the type locality in the Victorian goldfields, Australia (Ulrich, 1869).

The Bi-bearing sulphides and sulphosalts are a complex group, including bismuthinite-aikinite derivatives, lillianites and andorites, pavonite homologues, members of the galena-matildite series and minerals in Bi–Pb–Te–S and Bi–Te–Se–S systems. The ordered derivatives of the bismuthinite–aikinite solid-solution series are Bi_2S_3–$CuPbBiS_3$, Bi_2S_3 ($n_{aik} = 0$, bismuthinite), $Cu_{0.5}Pb_{0.5}Bi_{1.5}S_3$ ($n_{aik} = 50$, krupkaite), and $CuPbBiS_3$ ($n_{aik} = 100$, aikinite), where n_{aik} is the short form of aikinite (x) – bismuthinite (100 − x). The derivatives comprise a range of one-, three-, four-, and five-fold superstructures based on the incremental Bi + □ (where □ is a vacant tetrahedral position) ↔ Pb + Cu substitution (Petříček and Makovicky, 2006, Topa et al., 2002). The mineral lillianite, $Pb_3Bi_2S_6$, from which the complex homologous sulphosalt accretional series is derived, comprises two separate branches of sulphosalts, the Pb-Bi-Ag lillianite branch and the Pb-Sb-Ag andorite branch (Makovicky and Topa, 2014). Within the structure of lillianites, Pb, Bi (Sb) and Ag replace one another following 2Pb ↔ Ag + Bi(Sb) (Makovicky and Topa, 2014). The pavonite ($AgBi_3S_5$) series is a heterochemical isostructural series of 'unit-cell twinned' structures, resembling the unit-cell-twinned lillianite (Kasatkin et al., 2020, Makovicky et al., 1977). This series has minerals in the system

Ag–Cu–Bi– Pb–S and the main substitution mechanism is 2Pb ↔ Ag + Bi (Makovicky et al., 1977). Five Bi-sulphosalt intermediate phases occur along a matildite-galena join in the (Bi + Sb)–(Ag + Cu)–Pb ternary system (Damian et al., 2008, Wang, 1999). The mineral species in the series mentioned above are too numerous to be listed here.

Bismuth can also be incorporated in the tennantite-tetrahedrite series, also known as fahlore. Bi-rich fahlore is, however, rare (Johnson et al., 1986) and no Bi-end member has been found in nature (Gołębiowska et al., 2012). The maximum Bi content in fahlore is 22 wt%, reported from the Wittichen area in the Schwarzwald ore district, Germany (George et al., 2017, Staude et al., 2010).

Secondary Bi minerals associated with U deposits include bismite and bismoclite. The term bismuth ochre, which refers to the yellowish oxidation crusts on bismuth minerals, refers to both the individual minerals (bismite and bismoclite) as well as to mixtures thereof. The secondary Bi mineral russellite is a mixed Bi-W oxide that occurs along the grain boundaries of altered wolframite (Fig. 1D). Russellite is typically associated with W ± Sn mineralisation in felsic igneous rocks (Badanina et al., 2006, Moles and Tindle, 2012). Russellite was first recorded in 1938, by its namesake British mineral collector Sir Arthur Russell, from jig ore concentrates at Castle-an-Dinas tungsten mine, in Cornwall (Hey, 1938).

4. Geochemistry

4.1. Hydrothermal geochemistry of bismuth

Bismuth mineralisation occurs over a range of temperatures and pressures. The low temperature of melting, and mobility in magmatic systems, contribute to its widespread presence in the crust. Although Bi-bearing minerals are typically magmatically derived, Ciobanu et al. (2006a) showed that these minerals can occur in a variety of hydrothermal systems irrespective of fluid source, provided that the correct physico-chemical parameters are present.

The most important Bi-complexes in geofluids are hydroxy complexes, mainly $Bi(OH)^{2+}$ and $Bi(OH)_3$(aq), with trigonal pyramidal coordination geometries (Brugger et al., 2016)). Although Bi(III) chloride and Bi(III) bisulphide complexes are potentially important in some settings, the nature and stability of these remain poorly constrained (Brugger et al., 2016, Kolonin and Laptev, 1982, Skirrow and Walshe, 2002). Bismuth (III) chloride complexes are expected to account for Bi mobility in acidic brines, and Etschmann et al. (2016) showed that Bi (III) most likely exists as a mixture of $BiCl_5^{2-}$ and $BiCl_6^{3-}$. The number of Cl coordinated to Bi(III) decreases with increasing temperature; at around 200 °C and above, Bi(III) is coordinated to three Cl atoms, most probably in a trigonal pyramidal geometry (Brugger et al., 2016). The high stability of Bi hydroxyl complexes and the active lone electron pair mean that Bi is soluble in low-density vapours and is often associated with Cu and Au. Experimental studies by Kruszewski and Wood (2009) showed that the vapour phase was more important than liquid phase for Bi solubility at 220 °C.

Experimental data (Sugaki et al., 1981) and compositional data for bornite in skarn sulphide ore from the Tunaberg copper deposits in Sweden (Dobbe, 1991) suggest the existence of Bi-rich bornite solid solutions (ss). Bornite ss can contain a maximum of 17.2 wt% Bi at 420 °C and the extent of the solid solution is higher at low sulfur fugacity (fS_2) (Cook and Ciobanu, 2001, Sugaki et al., 1981); at 300 °C bornite contains a maximum of 2.3–3.4 wt% Bi (Dobbe, 1991, Sugaki et al., 1981). Below this temperature, trace elements in the Bi-rich bornite solid solution exsolve, resulting in mineral inclusions such as wittichenite. This has also been shown to occur in bornite ores in pegmatite at Mangualde, Portugal (Oen and Kieft, 1976), and in shear zone hosted bornite-bearing Cu-Au-Ag mineralisation at Glava, Sweden (Cook et al., 2011, Oen and Kieft, 1984).

Bismuth mineralisation occurs in high- to low-temperature systems (Section 5) and has a crucial role in controlling the Au deportment and tenor in Au-bearing deposits. Tellurides are common in high grade Au ores, for example the 200 g/t Au bonanza pipes of the Kochbulak epithermal Au deposit, Uzbekistan (Plotinskaya et al., 2006). The association is probably controlled by Au, as well as telluride and Bi-chalcogenide/sulphosalt- precipitation, being driven by the same abrupt and/or sustained fluctuation in physical-chemical parameters, irrespective of the fluid source (Ciobanu et al., 2006a, Ciobanu et al., 2009).

4.2. Bismuth-gold collector model

Bismuth melts are efficient scavengers of Au (Ciobanu et al., 2006a, Ciobanu et al., 2005, Cockerton and Tomkins, 2012, Douglas et al., 2000, Tooth et al., 2008, Tooth et al., 2011, Wagner, 2007) and this explains the strong paragenetic association between Au and Bi. The relationship is partially due to an overlap in the temperature of formation of Au deposits and the melting of native Bi and Au–Bi–Te–(S) assemblages (Ciobanu et al., 2010).

The Bi collector model describes a process whereby, at low sulfur fugacity, hydrothermal fluids over a broad temperature range >271 °C can melt native bismuth (Douglas et al., 2000). The resultant melt effectively strips Au from hydrothermal fluids to form Au-Bi melts (Tooth et al., 2008, Tooth et al., 2011, Wagner, 2007) which can contain up to 20 wt% Au (Cockerton and Tomkins, 2012, Douglas et al., 2000). Bismuthinite is a less effective potential Bi collector under most conditions as it has a much higher melting temperature of 775 °C (Lin et al., 1996).

Very low concentrations of Bi melt in the ore system (10–100 ppm) can scavenge Au from hydrothermal fluids, and so potentially contribute to Au enrichment (Tooth et al., 2011). Although incorporation of Au in Bi melts is more likely at high-temperatures (>400 °C) it has been argued that the process could operate also at low temperatures (Buzatu et al., 2015, Ciobanu et al., 2006a, Damian et al., 2008). The availability of native Bi and/or Au-Bi-Te-(S) minerals, and the temperatures and low sulfur fugacity of hydrothermal fluids are therefore controlling parameters for Au extraction (Douglas et al., 2000, Tooth et al., 2011). A Au-bearing Bi melt can exist down to the eutectic temperature (241 °C) of the Au-Bi binary system (Fig. 2), and possibly lower temperatures in the presence of other components (Cockerton and Tomkins, 2012, Tomkins et al., 2007). Experimental work has shown that the addition of Bi to a melt enriched in gold lowers melting temperature from 1064 °C to approximately 375 °C at atmospheric pressure (Tomkins et al., 2007). Native Bi + gold is the typical eutectic assemblage (Fig. 2).

A key mineralogical proxy for Au-bearing Bi-melts is the coexistence

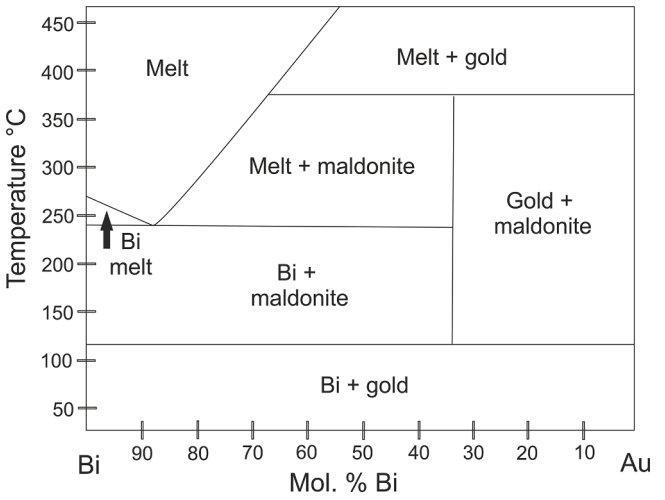

Fig. 2. Binary phase diagram in the system Bi-Au (after Tooth et al., 2008). Maldonite is Au_2Bi.

of maldonite (Au_2Bi) with native bismuth (Ciobanu et al., 2010, Ciobanu et al., 2005, Ciobanu et al., 2002). Maldonite and native bismuth crystallise from melt droplet inclusions, and exhibit curviplanar boundaries with one another and the hydrothermal mineral assemblage (Cepedal et al., 2006, Ciobanu et al., 2005). The existence of a bismuth melt in greisen deposits was inferred by Guimarães et al. (2019) who described trails of μm-sized blebs of native bismuth in cassiterite-quartz veins from the Santa Bárbara greisen Sn deposit in northern Brazil. At the NICO Iron-Oxide-Copper-Gold (IOCG) deposit in the North West Territories, Canada, the presence of Bi-Au inclusions in arsenopyrite supports enhanced Au concentration by the bismuth collector process (Acosta-Góngora et al., 2015a, Acosta-Góngora et al., 2015b).

The Bi-collector model has been invoked to explain Au deposition in mineral deposits of magmatic affiliation. Examples of this process can been seen from the epithermal-porphyry transition at Larga, Romania (Cook and Ciobanu, 2004), in Au skarns at Ortosa and El Valle, Spain (Cepedal et al., 2006) and Punta del Fanaio, Italy (Dini and Orlandi, 2010), in reduced intrusion-related gold deposit veins at Pogo and Fort Knox, Alaska (McCoy, 2000), in recent volcanogenic massive sulphide (VMS) systems, Escanaba Trough, Southern Gorda Ridge (Törmänen and Koski, 2005), and in orogenic veins in the Viceroy and Harare deposits, Zimbabwe (Oberthür and Weiser, 2008). Evidence from the Stormont prospect, Australia, shows the efficacy of the bismuth collector model, where fluctuating hydrothermal conditions allowed for the continued dissolution and reprecipitation of Au (Cockerton and Tomkins, 2012). Even in these highly gold-undersaturated fluids, the Bi melt continually scavenged Au, resulting in upgrading of the Au content (Cockerton and Tomkins, 2012).

Bismuth-dominated melts can also play a role in scavenging gold during regional metamorphism, e.g. upper greenschist facies, 400 °C; the estimated conditions for Alpine Au-Bi-S remobilisation from the Highiş Massif, Romania (Ciobanu et al., 2006a), if partial melting of pre-existing ore occurs during deformation (Ciobanu et al., 2010, Ciobanu et al., 2009, Tomkins et al., 2007).

4.3. Bismuth as an indicator of physico-chemical conditions

Bismuth minerals are valuable indicators of the physico-chemical conditions of mineral deposit formation, due to their sensitivity to changes in temperature, Eh–pH and oxygen, sulfur and tellurium fugacity (Afifi et al., 1988a; Afifi et al., 1988b; Cepedal et al., 2006, Ciobanu et al., 2010, Cook and Ciobanu, 2004, Foord et al., 1988, Meinert, 2000, Oberthür and Weiser, 2008, Tooth et al., 2008, Voudouris et al., 2013, Zhang et al., 2015, Zhou et al., 2016). This is further supported by the anomalous D value for Bi (Christy 2015) (section 2; Table 2).

In some instances, the Bi content of specific minerals can be used as a proxy for a range of depositional processes. For example, the trace element composition of galena is an indicator of temperature of deposition, where lower Sb:Bi ratios indicate higher temperature of crystallisation (Foord et al., 1988). Certain Bi minerals can be used to constrain the temperature of formation, for example at the Roter Bär deposit in the St. Andreasberg polymetallic vein district in the Harz Mountains, Germany, the presence of bohdanowiczite ($AgBiSe_2$) along with umangite (Cu_3Se_2) constrains the formation temperature to ≤ 120 °C (Cabral et al., 2017).

The anomalously high/maximum Bi content of hedleyite (~83–88 wt%), pilsenite (~71–72 wt%) and bismuthinite (approx. 80 wt%) from the Martinovo Fe skarn in Bulgaria is evidence for a low Te fugacity in the hydrothermal fluids (Dimitrova and Kerestedjian, 2006). An empirically-derived relationship between the Bi:Te(+S, Se) ratio and oxidation state in the tetradymite (Bi_2Te_2S) system was identified by Ciobanu et al. (2010). Minerals with a Bi:Te ratio >1 are associated with a reducing environment, where pyrrhotite and magnetite are the stable iron minerals. Minerals with a Bi:Te ratio <1 are associated with oxidising environments and the presence of pyrite and hematite. In the Nucleus-Revenue and Sonora Gulch intrusions (Tintina Gold Province) in the Yukon, Bi:Te(+S, Se) ratios suggest that mineralisation was associated with a reduced intrusion that contributed to the efficacy of the Bi-collector mechanism (Chapman et al. 2018).

Au skarns such as the Ortosa deposit in the Rio Narcea Gold Belt, Spain, have associated Bi-Te(-Se) phases (Cepedal et al., 2006). Gold occurs as native gold and maldonite, with pyrrhotite and arsenopyrite (as a replacement of löllingite), indicating low fO_2 conditions for Au mineralisation (Cepedal et al., 2006). This is supported by the speciation of Bi-tellurides and selenides (hedleyite, joséite-B, joséite-A, ikunolite-laitakarite) with a Bi-Te(Se + S) ≥ 1 (Cepedal et al., 2006). Thus, the speciation of Bi-bearing minerals is significant.

4.4. Bismuth in the surface environment

Data on Bi solubility in natural environments are few. However, the element appears soluble under acid conditions but becomes less mobile as pH increases (Hale, 1981). The principal valence states of Bi are 0 and +III under normal conditions. The bismuth(III) hydride (BiH_3) will only form under extremely reducing conditions (E^o (standard potential) = -0.97 V) and is thus very unstable. Bi(V) is highly oxidising, being able to oxidise water to oxygen (E^o = +2.1 V) (Kyle et al., 2011, Smith, 1973). The Eh-pH diagram (Fig. 3) shows that the oxide Bi_2O_3 occupies much of the Eh-pH field above the sulphide-sulfate boundary, and is replaced by $Bi_6O_6^{6+}$ at pH 5.5–6 for activites of dissolved Bi of 10^{-6} and 10^{-8}, respectively. Under sulphide-sulphate conditions, Bi_2S_3 (bismuthinite) occupies most of the Eh-pH space with native bismuth appearing at high pH and reducing conditions (Brookins, 1988).

These observations explain the frequent reports of bismuth ochres formed by near-surface weathering of Bi ores. The products of oxidation are bismite and Bi hydrocarbonates, vanadates and rarely silicates

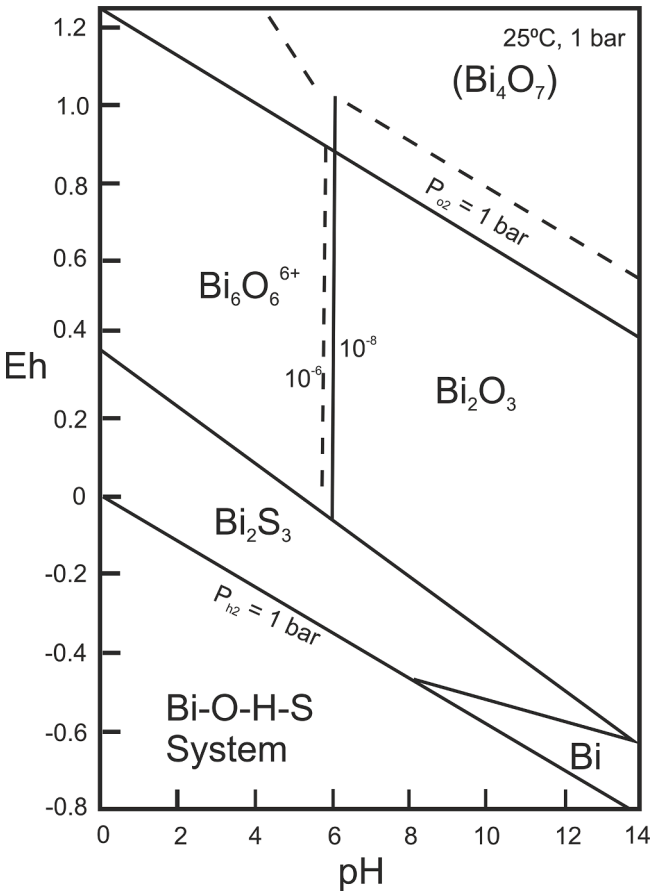

Fig. 3. Eh-pH binary plot for the Bi-O–H-S system (after Brookins, 1988).

(Angino, 1979). Testa et al. (2016) reported the occurrence of bismoclite and preisingerite (a bismuth oxy-arsenate) from the weathered zone of a Cu-rich polymetallic tourmaline breccia in Andean Argentina. If iron oxyhydroxide precipitation is common, then Bi may be incorporated into those phases, as evidenced by a number of weathering studies in Western Australia (Smith and Perdrix, 1983).

The Bi-rich end members of the tennantite-tetrahedrite series (fahlore) play an essential role in managing heavy metal release (Sb and As) during weathering (Keim et al., 2018). Where sufficient Bi is present in the weathering minerals, both As and Sb remain environmentally immobile. Conversely, where insufficient Bi is present, the heavy metals are released. Bi is fractionated during weathering and is more stable than either Sb or As. Keim et al. (2018) indicate that Bi released from sulphides by weathering is captured in oxide minerals that are stable in near surface environments. However, it has also been shown that Bi, along with other metals, in suspended mine waste dust in the Rio Tinto mining district of Andalusia, Spain, contributes 32% of the total concentrations of trace metals into the atmosphere (de la Campa et al., 2011).

4.5. Bismuth as a pathfinder in mineral exploration

There has been very little exploration for Bi as a primary commodity, but the element is used as a pathfinder for other deposits. This use has become routine, and less costly, with the advent of multi-element packages, using an ICP-MS or high sensitivity XRF finish, that allow precise determination of Bi at background crustal concentrations. Bi is most commonly used as a pathfinder element for Au mineralisation, along with Te, As, Sb, Hg, Se and Co (Hale, 1981, Phillips and Powell, 2015).

Bi-rich magnetite mineralisation is a potential indicator of Au mineralisation in skarn systems. The occurrence of Au with oxide minerals such as magnetite is incompletely understood but recent work by Zhou et al. (2017), Zhou et al. (2021) shows that a Bi melt can scavenge Au during magnetite growth from a hydrothermal fluid. Where external thermodynamic conditions such as oxygen fugacity or temperature are changing on the surface of the crystallising magnetite, it can trigger the dissolution-reprecipitation of magnetite, precipitation of Au-Bi and incorporation of Au and Bi minerals within the pores of magnetite (Zhou et al., 2017; Zhou et al., 2021).

Polymetallic veins and polymetallic replacement deposits sometimes have geochemical signatures and sulphide mineral assemblages similar to those of Au-bearing skarns, for example, the Fe-As-Zn-Cu-Bi-Au- and Sb-bearing ores at the Matsuo Mine, Japan (Matsukuma, 1961), may be high-level or lateral reflections of Au-bearing skarns and allow vectoring towards them (Theodore et al., 1991). Anomalous concentrations of Bi, Te, As, Se, and Co in soil and stream surveys are useful geochemical signatures for some Au-bearing skarns (Theodore et al., 1991).

Localised enrichment of Bi is an indicator of Au at the Hamlet orogenic Au deposit, Western Australia (section 5.9). Here a correlation between Bi and Au is used to identify fluid pathways and hence the distribution of the Au in the system (Hood et al., 2019). Bismuth minerals have also been considered pathfinders for Au in the stringer zones of VMS systems in the Iberian Pyritic Belt (Marcoux et al., 1996).

The Bi-Pb-Te-S mineral inclusion signature identified in detrital Au from porphyry systems persists into the associated epithermal signature. This has significant implications for Au exploration as the epithermal signature can be more regionally extensive than the geochemical signature for the porphyry alone (Chapman et al., 2018). The use of microchemical signatures in placer Au mineralisation can also be used to distinguish Au derived from porphyry systems from Au with an orogenic or multi-source origin. Mineral inclusion assemblages for the system Bi-Pb-Te-S (±Sb) can be determined in Au particles from multi-source placer deposits (Chapman et al., 2018). These assemblages comprise galena, bismuthinite, galenobismutite and arsenopyrite, or minerals that contain most or all of these elements (Bi-Pb-Te-S-Sb). There is a pronounced mineralogical association of the Bi-Pb-Te-S system mineral inclusions with calc-alkalic porphyry systems, and associated epithermal mineralisation, compared with the simple sulphides, sulfarsenides and more rarely sulphosalts and tellurides associated with Au formed in orogenic settings. This difference is a beneficial discriminator between Au sources for placer and detrital Au (Chapman et al., 2018). Where placer Au is intergrown with Bi minerals, including bismuth oxides or bismuth tellurides, it can be a downstream indicator of the presence of a Au-bearing skarn (Theodore et al., 1991).

5. Bismuth deposits

Bismuth is typically recovered as a by-product of Pb, W, Cu or Au mining, with extraction methods dependent on the ore mineralogy. In many cases, however, Bi is not recovered when it is in association with more abundant ore metals. The main deposit types where significant Bi mineralisation occurs (Fig. 4) are:

1. Skarn
2. Granite-related vein and greisen
3. Reduced intrusion-related Au-Bi
4. Porphyry-related
5. Iron oxide copper gold (IOCG)
6. Pegmatite
7. Five-element vein (Co-Ni-Bi-Ag-As ± U)
8. Orogenic gold
9. Volcanogenic Massive Sulphide (VMS): modern and ancient
10. Sediment-hosted copper

Deposits discussed here have previously been mined for Bi or are being explored with Bi as a noted by-product of that deposit. Examples where Bi plays an important role in the genesis of these deposits are also included where possible. Galena-dominated ore deposits are the most important for current Bi production. Bismuth can occur as inclusions of Bi minerals in galena, by isomorphous substitution of Pb^{2+} by Bi^{3+} (Wasserstein, 1951) or by coupled substitution of $2Pb^{2+}$ with $Bi^{3+} + Ag^{+}$ (Foord et al., 1988). There is a wide range in Bi content of galena across different deposit types (Fig. 5).

5.1. Skarn deposits

Skarns are formed by the metasomatism of the contact zone between an igneous intrusion and host carbonate lithologies. Skarns are mined globally for a variety of metals including Au, Cu, W, Fe and base metals (Meinert, 1992) and consistently high Bi content occurs in skarn-hosted galena.

The Shizhuyuan deposit in China comprises proximal skarn and greisen W–Sn–Mo–Bi and distal Pb–Zn–Ag veins, hosted by Devonian limestone in the thermal aureole of the Qianlishan granite complex (Lu et al., 2003, Mao et al., 1996, Wu et al., 2018). It hosts significant amounts of Bi as bismuthinite and it is one of the few deposits where Bi is mined as a by-product. Zhong et al. (2017) report the deposit as hosting 0.2 Mt at a grade of 0.19 % Bi. There are three Bi parageneses: retrograde skarn, later massive greisen ore, and stockwork, with overprinting relationships common across the deposit (Lu et al., 2003). Bismuthinite is predominantly hosted in the retrograde skarn stage of mineralisation (Lu et al., 2003). Galena in the distal Pb-Zn-Ag veins has low Bi content (0.02–0.08 wt%) (Wu et al., 2018) (Fig. 5, locality 12), even though the overall system is enriched. This is likely due to the early crystallisation of bismuthinite in the intrusion-related mineralisation system, with Bi-depleted fluids forming the base metal vein-hosted deposits (Wu et al., 2018). Another Pb-dominant skarn example with high concentrations of Bi in galena is the Lamo deposit in the Dachang ore field, Guangxi, China that has average Bi values >12 wt% in galena (Xilin, 1990). In the Mozumi skarn-type Zn-Pb-Ag deposit of the Kamioka mine, Japan, one of the largest skarn deposits globally, Bi is incorporated into galena (up

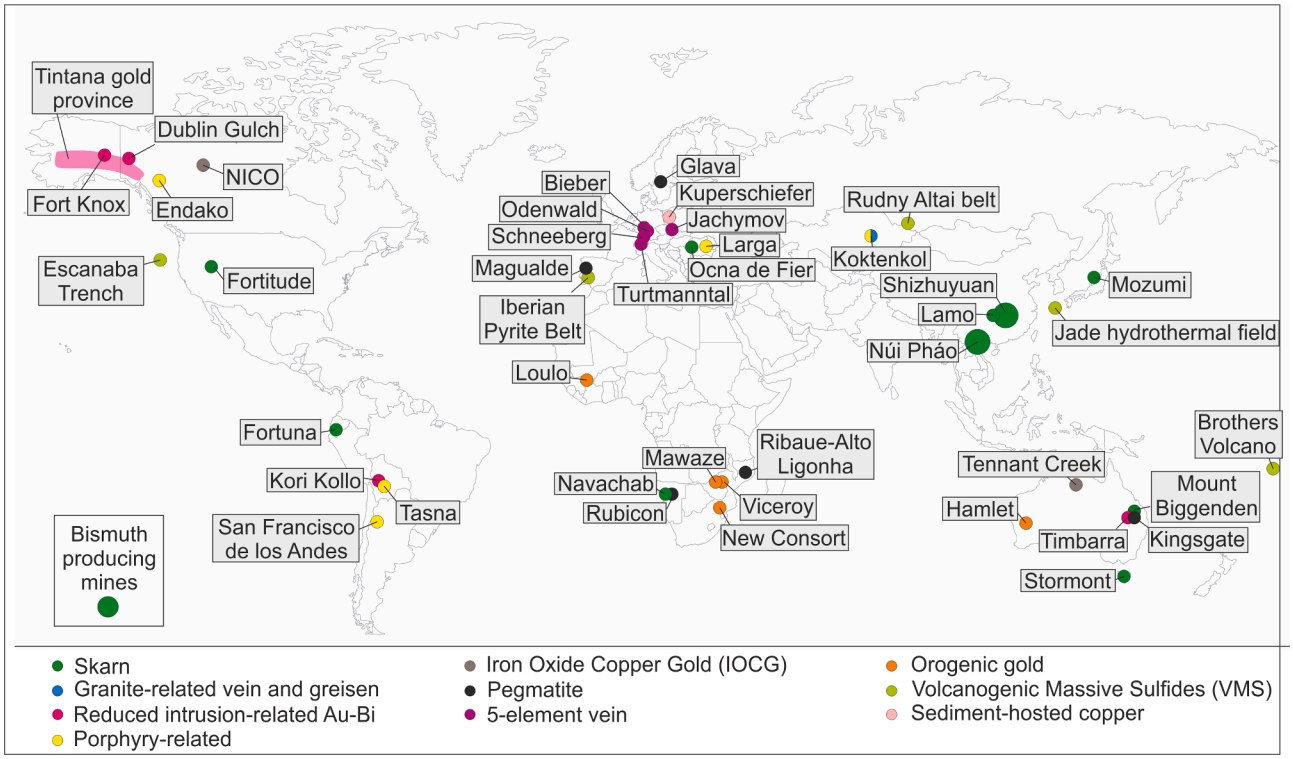

Fig. 4. The distribution of Bi deposits and occurrences mentioned in the text.

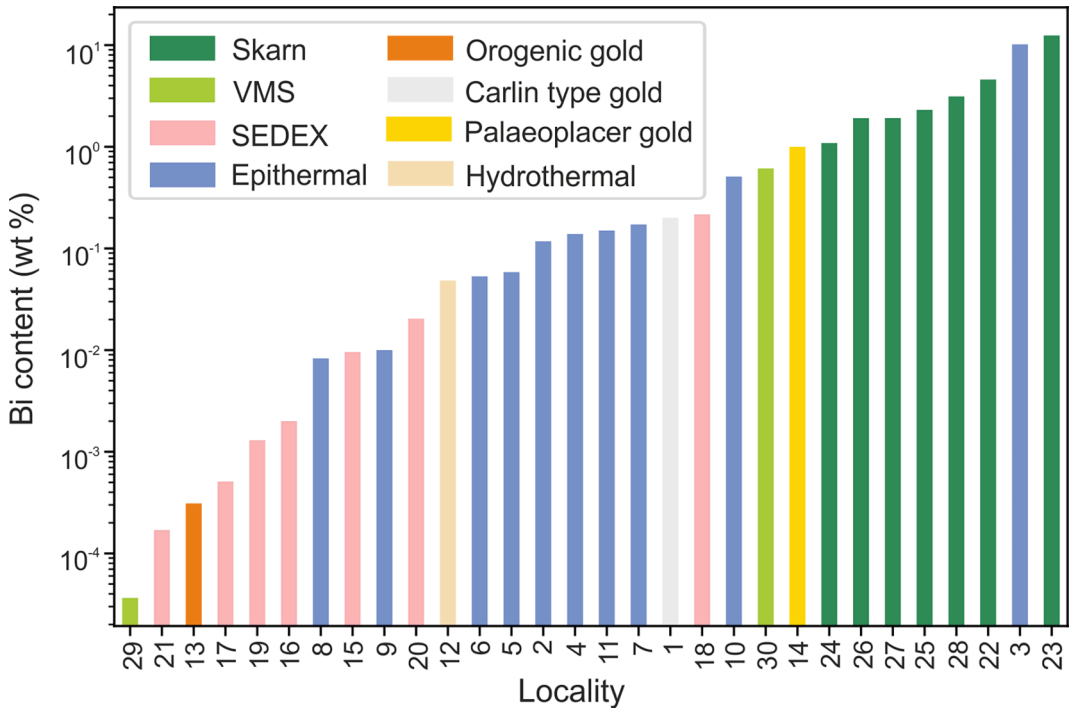

Fig. 5. Range of Bi content in galena from different deposit types, data from 29 individual locations. (Locality references: 1, 10, 11, Foord et al., 1988; 2, Graeser 1969; 3, Groznova et al., 2005; 4–8, 13, 15–21, 24, 29, George et al., 2015; 9, 14, Wasserstein, 1951; 12, Wu et al., 2018; 22, Gvozdev, 2009; 23, Xilin, 1990; 25–26, Simanenko, 2007; 27, Mariko et al., 1996; 28, Ciobanu and Cook, 2000; 30, Grant et al., 2015). Full data on the localities are compiled in supplementary file 1.

to 3.89 wt%) by coupled substitution with Ag (Mariko et al., 1996).

Núi Pháo, a world-class polymetallic W-F-Cu-Au-Bi deposit in northern Vietnam, provides an excellent case study of a skarn that hosts Bi mineralisation. Whilst Bi is a by-product of W production, it is the first major Bi-producing mine to open (Fig. 6A) since the closure of the Tasna mine in Bolivia in 1985. The average grade is 0.108% Bi, based on a 0.2% WO_3 equivalent cut-off (Hau et al., 2020; Richards et al., 2003) and there are large estimated resources. Production commenced in 2014 and, within two years, surpassed that of China, although production levels dropped again in 2019 (Brown et al., 2021). Ordovician to

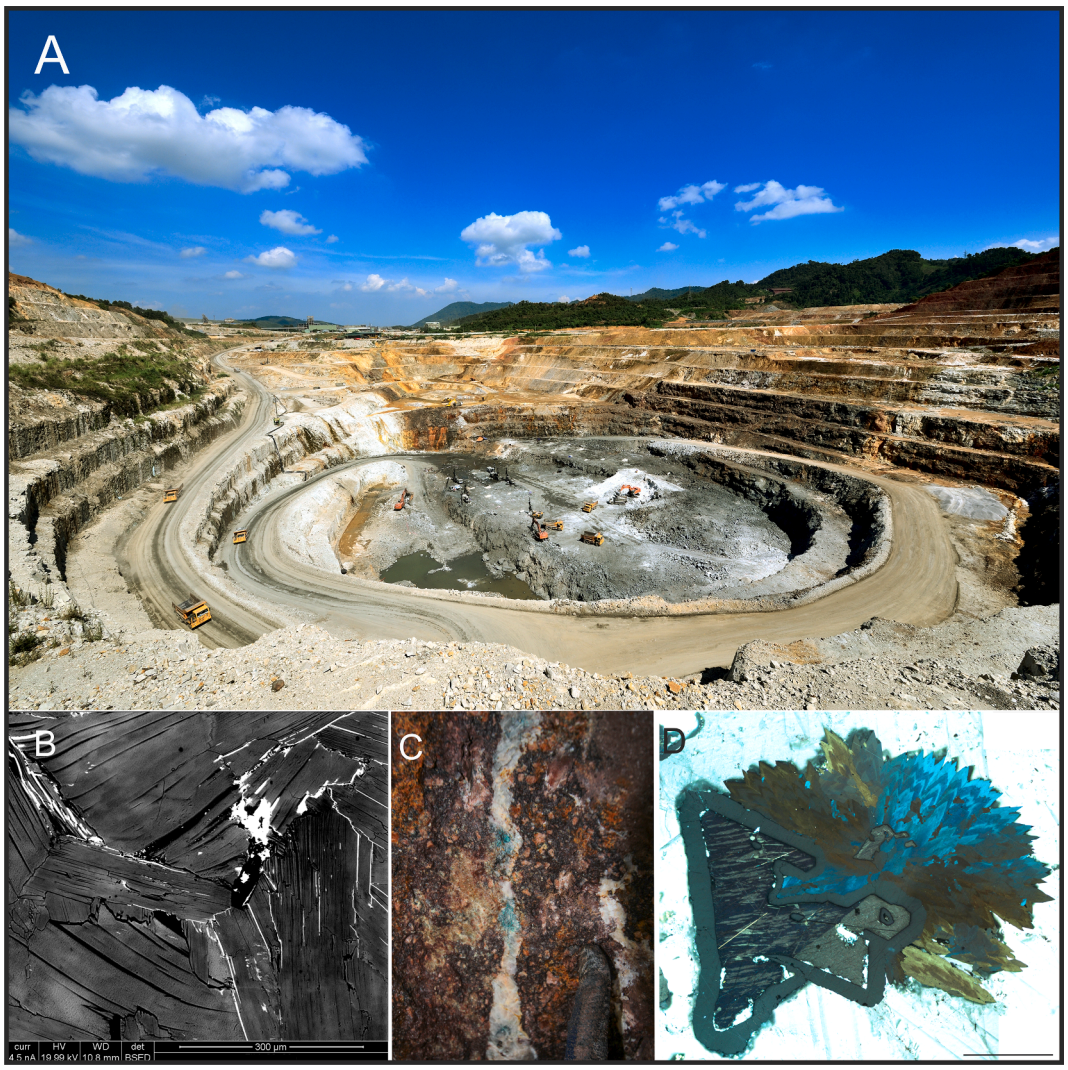

Fig. 6. A. Overview of production at the Núi Pháo mine 2020. Image courtesy Masan Resources (section 5.2). B. Native bismuth in the cleavage of mica in the Arcadia LCT-type pegmatite in Zimbabwe. Image courtesy Richard Shaw. C. Five-element vein mineralisation from the Schwartzwald, Germany. Cu-Bi secondary minerals (green) in a quartz vein (approx. 1 cm wide) in altered granite. Image courtesy Manuel Scharrer. D: Secondary zoned Cu-Bi minerals after chalcopyrite (PPL). Scale is 1 mm. Image courtesy Manuel Scharrer.

Silurian sedimentary lithologies, intruded by the Triassic Núi Pháo biotite granite, 244 Ma (Hau et al., 2020), and the Late Cretaceous two-mica Da Lien granite, 82.8–82.5 Ma (Ishihara and Orihashi, 2014; Richards et al., 2003; Sanematsu and Ishihara, 2011), host the steeply-dipping deposit that comprises greisen veins and skarn assemblages (Hau et al., 2020; Richards et al., 2003). The mineralised zone extends ~1500 m E-W and its thickness varies from 300 to 400 m (Hau et al., 2020). Skarn assemblages host mineralisation comprising scheelite, pyrrhotite, native bismuth, and chalcopyrite (Hau et al., 2020). Mineralisation at Núi Pháo occurred over three stages, with the majority of the Bi mineralisation occurring during the main ore-forming stage associated with a retrograde skarn assemblage (Hau et al., 2020). The early skarn was subsequently overprinted by fluids from the Da Lien granite which resulted in pyrrhotite-fluorite-albite skarn and greisen that host significant fluorite mineralisation (Hau et al., 2020), along with W (as scheelite) and Bi (as native bismuth and bismuthinite) mineralisation (Masan Resources, 2016; Richards et al., 2003).

At Stormont, Tasmania (Australia) a number of Au-Bi skarn deposits occur within a gently folded sequence of fractured and faulted fluorite-magnetite-garnet skarns. The skarns formed in the Moina Sandstone and the Gordon Limestone formations following emplacement of the Dolcoath Granite. Gold is closely associated with bismuthinite in an andradite garnet skarn developed above a Au-Bi depleted magnetite skarn. The Stormont Bismuth Mine historically produced 6.3 tonnes Bi (1928–1934) contained in concentrates averaging 63% Bi and 450 g/t Au. Gold was a by-product recovered during bismuthinite concentrate production in a simple crushing-grinding-gravity mill. Stormont has an inferred resource of 0.151 Mt at 0.17% Bi, 2.89 g/t Au and 3.82 g/t Ag (at a cutoff grade of 0.5 g/t Au) (Skirrow et al., 2013).

Bismuth minerals, such as bismuthinite and native bismuth, are reported in 23% of global Au-dominant skarn deposits and in 9% of skarn deposits where Au is a by-product (Meinert, 2000; Theodore et al., 1991). Gold-bearing skarns can develop in either reduced or oxidised environments (Meinert, 2000; Theodore et al., 1991). Bismuth has a stronger association with those formed in reduced environments, characterised by sulphides and As mineral assemblages, e.g. Fortitude, United States (Theodore et al., 1991), Fortuna, Ecuador (Markowski et al., 2006) and Navachab, Namibia (Dziggel et al., 2009; Nörtemann, 1997), than in oxidised Au-bearing skarns (Meinert, 2000). One notable oxidised Au skarn is the Mount Biggenden Au-Bi (-magnetite) deposit in Australia, where significant Bi ore (bismuthinite and native bismuth) was extracted historically (Seccombe et al., 2005; Theodore et al., 1991).

Bismuth also occurs as Bi-bornite and Bi-Au solid solutions in skarn,

such as in the exoskarn at the Wombat Hole Prospect, Victoria, Australia (Henry and Birch, 2022). Gold typically occurs as electrum and is closely associated with Bi and telluride minerals such as native bismuth, hedleyite, wittichenite and maldonite (Meinert, 1992). Most native bismuth in skarn and veins is >99 mol.% Bi. However, at the Navachab reduced Au skarn deposit in Namibia, native bismuth in some of the skarn samples contains up to 4 mol.% Au in solid solution (Nörtemann, 1997; Nörtemann et al., 2000).

In the chalcopyrite ore of the Simon Luda orebody at the Ocna de Fier high temperature skarn deposit (Romania), wittichenite is the most common Bi mineral, exsolved directly from bornite during prolonged cooling; in the Fe skarn part of the deposit Bi deportment is primarily across a complex range of Ag-Pb-Bi and Cu-Pb-Bi-sulphosalts (Ciobanu and Cook, 2004).

5.2. Granite-related vein and greisen deposits

Bismuth is associated globally with proximal zones of granite-related W and Sn deposits, in both B-(tourmaline) and F-rich granites (Rundquist, 1982) (Fig. 1B, D), where it occurs as, usually minor, native Bi and bismuthinite in greisen and vein systems (Elliott et al., 1995). Evidence for Bi melts in greisen systems of Precambrian age, 0.99 Ga (Bettencourt et al., 2016)) comes from the Santa Bárbara greisen Sn deposit in northern Brazil (Guimarães et al., 2019), where blebs of Bi melt are trapped as trails along crystal growth zones in cassiterite. The Mount Pleasant complex in New Brunswick, Canada hosts significant greisen-hosted mineralisation. Historically mined for Mo, initial resource estimates (1971) indicated 22.5 Mt at 0.08% Bi in greisen veins that occur in the contact zone between fine-grained granite and a quartz feldspar porphyry (Kooiman et al., 1986; Parrish and Tully, 1978). Bismuth occurs mainly as the native metal, and less commonly, as bismuthinite typically with arsenopyrite veinlets, and sporadically intergrown with, or attached to, wolframite grains (Davis and Williams-Jones, 1985). The Mo-rich greisen deposit at Koktenkol in Kazakhstan hosts Mo-W-Bi mineralisation in a distal stockwork system where the main Bi ore mineral is bismuthinite (Kotlyar et al., 1995). Some authors choose to classify the deposit as porphyry Mo (John and Taylor, 2016) despite the variety of greisen, porphyry, stockwork and overlying skarn assemblages that are associated with mineralisation (Kotlyar et al., 1995; Figs. 3-7). The bismuth mineralisation in the deposit, hosted in minerals of the bismuthinite-aikinite series and as native bismuth, was considered significant enough to extract, although the project was abandoned in the 1980s (John and Taylor, 2016; Mazurov, 1996).

Many Variscan (late Devonian – early Permian) associated granite-greisen systems also host Bi mineralisation, including parts of the Bodmin Moor, Bosworgy (Ball and Basham, 1984) and Hemerdon granites of the Cornubian Batholith, UK (Fig. 1B and D), the Podlesí granite system (Breiter et al., 2006), the Vykmanov and Boží Dar granites in the western part of the Krušné hory pluton, Czech Republic (Štemprok et al., 2005) and Panasqueira, Portugal (Polya, 1989; Wimmers, 1985). Some vein Sn deposits in Cornwall, south west England are also Bi-rich, notably Wheal Jane, in which a greisen phase is overprinted by later sulphides (Kettaneh and Badham, 1978; Rayment et al., 1971).

Evidence for the introduction of a new Bi-bearing fluid or remobilisation of earlier Bi by later stage hydrothermal fluids comes from the occurrence of secondary Bi- minerals. Secondary Bi minerals, bismutite and russellite, have been recorded in greisen veins in the Paleocene Mourne Granite Complex in Northern Ireland, UK (Moles and Tindle, 2012), and in wolframite-quartz veins from the Castle-an Dinas tungsten deposit in south-west England (Hey, 1938).

5.3. Reduced intrusion-related Au-Bi systems

A smaller class of Au deposits, with a distinct associated metal assemblage that includes Bi, are the intrusion-related Au systems (IRGS). The classification is notoriously challenging, due to overlapping characteristics with other deposit types such as orogenic gold deposits and the influence of varying redox conditions. Here we refer to (Hart, 2005; Hart, 2007; Thompson et al., 1999) to describe the reduced-IRGS (RIRGS) deposit type. These are genetically related to granitoid intrusions, with elevated Bi, W, As, Mo, Te and/or Sb, with low associated concentration of base metals. These are spatially restricted, with weak alteration, and associated with low salinity carbonic and aqueous-carbonic hydrothermal fluids, and a low sulphide mineral content. They are distal to convergent plate boundaries, and in areas of known W-Sn mineralisation. Mineralisation typically occurs in sheeted vein

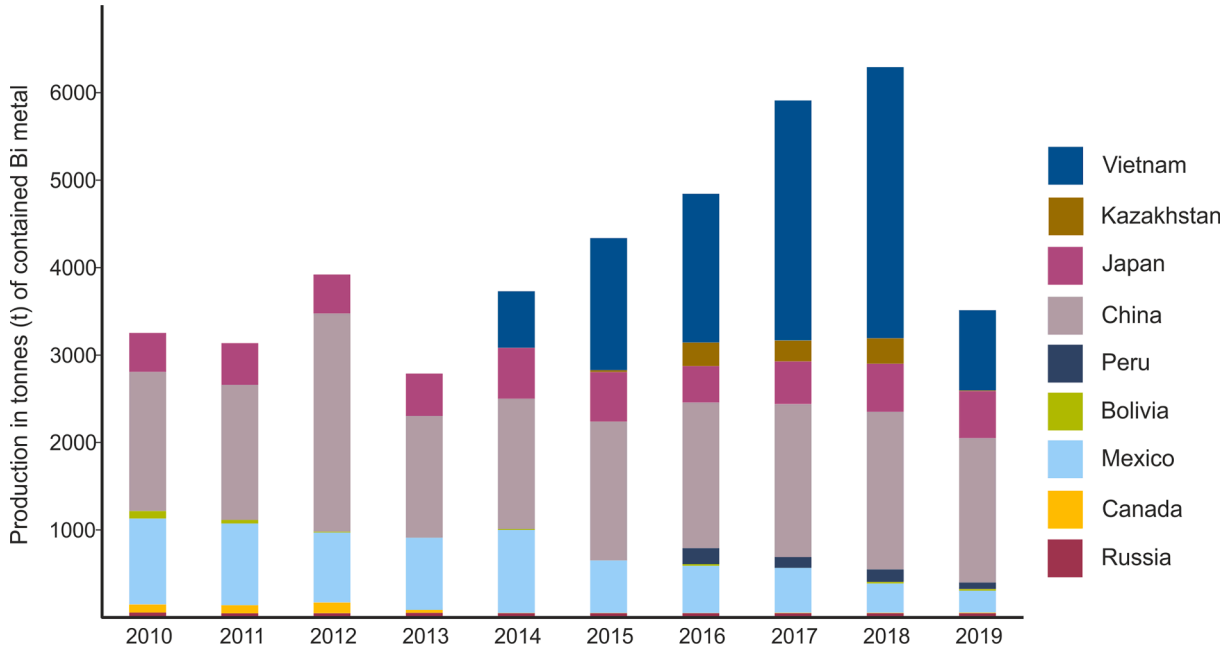

Fig. 7. Bismuth production by producing country from 2009 to 2019. Data from the British Geological Survey (Brown et al., 2021), 2019 is the most recent year for which data exist. Production also occurred in Armenia and Bulgaria during this period but are too small to be seen clearly on the graph. The full data for this graph are in supplementary file 1.

systems although brecciated, greisen-like and disseminated mineralisation have all been described (Thompson et al., 1999). In RIRGS deposit types, Bi, along with Au-Ag-Te-S, occurs as maldonite and as Bi-tellurides (e.g., tellurobismuthite, tetradymite, hedleyite, joséite-B, joséite-A and pilsenite). For example in Fort Knox, USA (McCoy, 1997), Vasilkovskoe, Kazakhstan (Bespaev et al., 1996), Timbarra, Australia (Baker et al., 2005), Kori Kollo, Bolivia (Long et al., 1992) and in the Tintina gold province, United States and Canada (Hart et al., 2000; McCoy, 2000). At Timbarra, free Au occurs with Pb-Bi and Ag-Bi tellurides (Mustard, 2001).

5.4. Porphyry-related deposits

Bismuth is enriched in some porphyry Mo and Cu deposits (John and Taylor, 2016). Significant enrichments appear confined to those of the Mo-W type, notably Endako in British Columbia. At Endako, the bismuth, as bismuthinite, is associated with Mo mineralisation in two types of quartz vein: stockwork and ribbon-textured (laminated) veins. The early stockwork veins are associated with intense Type A K-feldspar alteration while the later stockwork veins are bordered with Types B and C K-feldspar alteration (Selby et al., 2000). Moderate to intense kaolinite alteration is related spatially to ribbon veins, overprinting the original sericite alteration assemblages (Selby et al., 2000). Bismuth at this deposit is considered an impurity and is not recovered (John and Taylor, 2016 and references therein). Bismuth is also associated with epithermal-porphyry systems, for example Larga, Romania (Cook and Ciobanu, 2004).

One of the few historical primary Bi producers, located in the Tasna district of Bolivia's Eastern Cordillera, near Potosi, is porphyry related. Mining here took place at the Sn-W-Bi deposits of Rosario, Matilde, Farelon Nuevo and Belen (Sugaki et al., 1988), which closed in 1985, but have *in situ* resources estimated at 500,000 metric tons, at 1.47% bismuth and 1.28% copper, with credits for Au, Ag, and W (U.S. Geological Survey, 1996). The mineralisation at Tasna occurs as Sn-W-Bi-Ag-Pb-Zn and Bi-Cu-Sn veins, hosted by hornfelsed sedimentary rocks, over several square kilometres. The mineralisation has been related to hypersaline metal-bearing magmatic fluids (Sugaki et al., 1988) exsolved from an underlying quartz porphyry (Grant, 1979).

5.5. Iron oxide copper gold (IOCG) deposits

The Paleoproterozoic NICO deposit, Canada, is a magnetite-dominated IOCG deposit, with Co-Au-Bi ± Cu-W mineralisation hosted in strata-bound lenses that occur in metasedimentary rocks of the Treasure Lake Group (Acosta-Góngora et al., 2015a). Bismuth mineralisation is paragenetically late, following the precipitation of Co-rich sulfarsenides, and is represented by native bismuth, bismuthinite and emplectite. Here, Bi is interpreted to have decoupled from the Co-Cu-W-bearing fluid as coeval magnetite precipitated, evidenced by native bismuth and magnetite ± bismuthinite veins cutting early mineral assemblages (Acosta-Góngora et al., 2015a, Acosta-Góngora et al., 2014; Acosta-Góngora et al., 2015b).

Au-Cu-Bi mineralisation is also associated with a Proterozoic-aged IOCG at the Tennant Creek goldfield in the Northern Territories of Australia. Here, mineralisation occurs in pipe-like, ellipsoidal and lens-like structures and lodes of magnetite and hematite that are hosted by turbidites (Zaw et al., 1994). It comprises ten major deposits and hundreds of smaller deposits (Zaw et al., 1994). The region is historically significant for Bi mining. Bismuth is typically hosted by a chemically diverse range of sulphosalts such as junite ($Bi_8Pb_3Cu_2(S,Se)_{16}$) and wittite ($Pb_9Bi_{12}(S,Se)_{27}$), members of the bismuthinite-aikinite series (Large, 1974), and sulphides (Skirrow, 2000).

5.6. Pegmatites

Bismuth minerals are often minor components in the more evolved pegmatites of the LCT (Li–Cs–Ta) and NYF (Nb–Y–F) types (Foord, 1996; Márquez-Zavalía et al., 2012). Although Bi concentrations are typically uneconomic, some have been exploited historically for bismuth. Minster (1979) outlined two main modes of occurrence of Bi in pegmatites, those dominated by native bismuth and bismuth associated with base metal sulphides, and Bi associated with Nb-Ta bearing pegmatites, as bismuthotantalite ($BiTaO_4$).

At the LCT-type El Quemado pegmatite at Salta, Argentina, late stage mineralisation resulted in the formation of an assemblage of Bi-rich, Te-bearing minerals. The assemblage includes native bismuth, bismuthinite, emplectite and hodrušite ($Cu_8Bi_{12}S_{22}$) (Márquez-Zavalía et al., 2012), the latter sulphosalt more typical of a hydrothermal assemblage and uncommon in granitic pegmatites (Koděra et al., 1970). This assemblage is restricted to relatively low temperatures and pressure in the range 2–3 kbar (Márquez-Zavalía et al., 2012). Late-stage or supergene alteration of this assemblage generated bismutite and rare bismite (Márquez-Zavalía et al., 2012). This pegmatite field produced >5 t of bismuth ore concentrates in the 1940s (Galliski, 1983; Márquez-Zavalía et al., 2012).

At the LCT-type Pala pegmatite complex that intrudes the Southern California Batholith, the more common Bi-minerals, native bismuth, bismuthinite, bismite, bismutite, and beyerite ($Ca(BiO)_2(CO_3)_2$), are found with the rare Bi minerals, clinobisvanite ($Bi(VO_4)$), eulytite ($Bi_4(SiO_4)_3$) and namibite ($Cu(BiO)_2(VO_4)(OH)$), in the quartz-rich cores of the pegmatites (Foord, 1996). Native bismuth, bismutite and other unidentified Bi-phases have been recognised in the Rubicon pegmatites in Karibib, Namibia (Baldwin et al., 2005), while bismutotantalite ($BiTaO_4$) has been found associated with the Nb-Ta rich pegmatites at Wampewo and Mbale, Uganda (von Knorring and Fadipe, 1981).

Supergene bismuth mineralisation in the form of bismutite, sometimes called 'bismuth ochre', has been identified in the weathered parts of several granite pegmatites from Mozambique (Sahama and Lehtinen, 1968). Native bismuth and bismuthinite was extracted from LCT-type pegmatites in the Ribaue-Alto Ligonha region of Mozambique (Bandy, 1951). A complex range of rare secondary bismuth minerals such as cannonite ($Bi_2(SO_4)O(OH)_2$), bismutoferrite ($Fe^{3+}{}_2Bi(SiO_4)_2(OH)$) and preisingerite ($Bi_3(AsO_4)_2O(OH)$) have been identified in the supergene zone of pegmatites in the Kingsgate region of New South Wales, Australia (Sharpe and Williams, 2004).

5.7. Five-element (Co-Ni-Bi-Ag-As ± U) vein deposits

Five-element vein deposits (Co-Ni-Bi-Ag-As ± U) are important sources of Bi ore in the form of native bismuth (Kissin, 1992). First observed at the 'Bi-Co-Ni Formation' at Erzgebirge, Germany (Oelsner, 1958), examples of this deposit type include the Wittichen and Clara mines (Schwarzwald) and St. Andreasberg (Harz Mountains), Germany, Bieber and Schneeberg (Erzgebirge), Germany, Jáchymov (Krušné hory), Czech Republic and Turtmanntal, Switzerland (Cabral et al., 2017; Markl, 2015; Markl et al., 2016; Ondrus et al., 2003). Typical mineralisation comprises metallic Bi, As and Ag with subsequent Co-Ni-Fe arsenides (e.g. Fig. 6B and C) (Cabral et al., 2017; Markl et al., 2016; Ondrus et al., 2003; Staude et al., 2012).

The major Jáchymov-Gera Fault zone is located to the north-east of the Erzgebirge/Krušné hory mountain range, stretching across the border of Germany and the Czech Republic. The region hosts significant Bi-Co-Ni mineralisation as well as U and Ag mineralisation. Combined production figures for Bi, Co and Ni (individual figures are unavailable) from the region are 15 thousand metric tonnes of metal (Seltmann and Štemprok, 1994; Štemprok, 1995). The Schlema-Alberoda (Aue) U deposits were explored and mined by the Wismut company to a depth of 2 km, near Schneeberg, Germany and are the best understood (Naumov et al., 2017). Bismuth occurs with Co and Ni minerals in late sulfur-poor ankerite veins, younger than quartz-calcite-uraninite and dolomite-uraninite veins. Five-element vein deposits in the Jáchymov ore district host significant Bi as native bismuth, with locally remobilised

veinlets of native bismuth present in fractures of the gangue minerals (Ondrus et al., 2003). Bismuth metal also occurs with skeletal or quill-like habit and more rarely as bismuthinite (Ondrus et al., 2003).

An alternative model of formation has recently been presented for five-element vein deposit types using mineralisation at Odenwald in south-west Germany as an example (Burisch et al., 2017; Markl et al., 2016). Native bismuth in these deposits characteristically occurs as large (up to several dm) aggregates that appear as 'floaters' in the gangue with little or no contact with the host rock (Markl et al., 2016). Ternary mixing of a deep-seated metal-rich basement brine (fluid A), a sulphide-bearing (H_2S and HS^-) basinal/sedimentary brine (fluid B) and methane-dominated fluid/gas (fluid C) induce ore formation (Burisch et al. 2017 and references therein). This invokes the interaction of a contemporaneous sulphide-dominated hydrothermal system with a strongly reducing fluid phase (liquid or gas) (Markl et al., 2016). Natural fracking of local host rocks is a potential source of the reducing hydrocarbons or hydrocarbon-bearing fluids. Evidence for the presence of these reductants comes from fluid inclusion microthermometry studies and carbon isotope analysis (Markl et al. 2016 and references therein). Mineral precipitation in a reductive environment is facilitated by the oxidation of CH_4 to CO_2 (Burisch et al., 2017).

5.8. Orogenic gold

Bismuth has a close association with Au in some orogenic gold deposits, with a characteristic Bi-Te (-Se) geochemical signature. At the Archean-aged Hamlet orogenic Au deposit, St Ives, Western Australia, localised Bi enrichment is correlated with Au and reflects the movement of reactive fluid through the shear zone that hosts gold (Hood et al., 2019). At the Viceroy Mine in the Harare–Bindura–Shamva greenstone belt, Zimbabwe, a wide range of Bi-bearing sulphosalts includes joésite-A, joésite-B, hedleyite, ikunolite and jonassonite, along with native bismuth, maldonite and bismuthinite. These minerals are interpreted as a possible epithermal overprinting of earlier orogenic Au mineralisation (Oberthür and Weiser, 2008). This potentially later Bi-Te-S overprint may have extracted some of the Au from pre-existing Au-bearing arsenopyrite, resulting in an upgrade of the Au ores (discussed in section 4.2) (Oberthür and Weiser, 2008). At the Mazawe mine, Zimbabwe, limited Bi occurs in association with Au. This is a pyrite-dominated assemblage and the Bi-Te-S phases at Mazowe reflect their sulfur-rich environment (elevated fS_2 buffered by pyrite combined with higher fTe_2), and have Bi/(Se + Te) ratios of 1 (Oberthür and Weiser, 2008). The presence of Bi is also noted at orogenic Au deposits such as New Consort Gold Mine, South Africa (Otto et al., 2007) and deposits in the Loulo mining district of Mali (Lawrence et al., 2013).

5.9. Volcanic-hosted massive sulphides: Modern and ancient

Seafloor massive sulphides (SMS), which form in modern back-arc spreading centres and submerged island arc volcanoes, are enriched in Bi, Cd, Ga, Ge, Hg, In, Mo, Sb, Se, Te, and Tl (Monecke et al., 2016) and in Zn, Pb, Au, Ag and As (Keith et al., 2016) when compared to Mid Ocean Ridge hydrothermal systems. Bismuth, In, Mo, Se and Te occur in highest concentrations in massive sulphides that are dominated by chalcopyrite (Monecke et al., 2016). Bismuthinite, tellurobismuthite, tetradymite and native bismuth are the most common Bi minerals in SMS and in their fossil analogues, volcanogenic massive sulphides (VMS) deposit types, with Bi contents of up to 500 ppm in VMS deposits (Monecke et al., 2016). Overall, the global Bi endowment of SMS deposits equals only 0.2% of the Bi reserves contained in land-based ore deposits (Monecke et al., 2016). However, it's important to consider that Bi reserve data are overall poorly constrained and there are limited data for Bi in SMS deposits.

Bismuth enrichment in pyrite in submarine hydrothermal systems is dependent on the lithologies with which the fluids interact (Keith et al., 2016). A significant fluid-rock interaction in lithologies that have crustal or sedimentary components, or where sedimentary constituents formed part of a subducting slab (Koski et al., 1988; Zierenberg et al., 1993), can produce a high Bi content in pyrite such as at the Jade hydrothermal field, Japan (up to 633 ppm) (Keith et al., 2016). The Brothers Volcano, in the southern part of the Tonga–Kermadec arc, also has elevated Bi content (up to 99 ppm) in pyrite (Keith et al., 2016). This is explained either by the transport of Bi in magmatic volatiles from the underlying magma chamber to the hydrothermal system (Berkenbosch et al., 2012; de Ronde et al., 2011; Keith et al., 2016) or the leaching of Bi from felsic arc rocks (Dekov and Savelli, 2004). The high bulk Bi content (>2000 ppm) in some of the chimneys in the Brothers Volcano (de Ronde et al., 2011) may be linked to the fact that this location has the highest known contents of Au (up to 40.4 wt% Au in chalcopyrite and up to 91 ppm Au in Bi-tellurides) of any submarine system (Berkenbosch et al., 2012). In contrast, where the slab component comprises altered basalts, as is the case at the northern part of the Tonga–Kermadec arc (Volcano 19 and Hine Hina), there is a low concentration of Bi in pyrite (Keith et al., 2016).

Sulphide-dominated samples from the Escanaba Trough, a recently active VMS system on the south Gorda Ridge offshore from northern California (United States), have elevated Bi concentrations >25 ppm (Benninger and Koski, 1987; Koski et al., 1994; Koski et al., 1988; Monecke et al., 2016). Gold mineralisation is controlled by the presence of Bi melt droplets hosted in the highly reduced fluids diffusing through mounds and chimneys associated with the late stages of vent activity. Gold in these fluids was scavenged by coexisting Bi melt droplets (Törmänen and Koski, 2005). Droplets of Bi melt in the voids between mineral grains have a greater control over gold deportment than refractory bismuth in late forming pyrrhotite (Törmänen and Koski, 2005).

Temperature-related minor element enrichment trends observed in modern sea-floor hydrothermal systems are broadly comparable to those encountered in Volcanogenic Massive Sulphide (VMS) deposits (Monecke et al., 2016). Where the paragenesis of VMS deposits is well described, approximately 15% record the presence of at least one Bi mineral (Monecke et al., 2016; Mosier et al., 1983). Bismuth, along with other heavy metals such as Sb and Cd, can occur as trace elements in chalcopyrite hosted by VMS. High Bi values are reported, or implied in many fossil VMS, notably those associated with felsic volcanism such as Rudny Altai in Russia and Kazakhstan (Eremin et al., 2007) and the Iberian Pyrite Belt (up to 5629 ppm) (Marcoux et al., 1996). Chalcopyrite from deposits in the Troodos Complex, Cyprus, has a widely varying Bi content from 0.06 to 506 ppm (Martin et al., 2019). Bismuth minerals such as bismuthinite and bismuth tellurides have been reported from VMS deposits in the Urals (Belogub et al., 2011; Maslennikov et al., 2017).

5.10. Sediment-hosted copper

Bismuth is known to be concentrated in black shale-hosted deposits such as the Kupferschiefer in the Lubin area of Poland. The smelter feed contains 7 ppm Bi and is potentially recoverable (KGHM Polska Miedź, 2019). Emplectite and cuprobismuthite ($Cu_8AgBi_{13}S_{24}$) have been recognised in Pd-Hg telluride veins in the strata-bound Cu-Ag mineralisation in the Kalahari copper belt in northwest Botswana (Piestrzyński et al., 2015).

6. The bismuth supply chain

6.1. Bismuth production

Although Bi has been the main economic product from some mines, such as Tasna in Bolivia, most Bi is a by-product of Pb and W extraction and processing. Annual global production in 2020 was 3700 tonnes, falling from a ten year high of 6300 tonnes in 2019 (Brown et al., 2021) (Fig. 7). Minor amounts of Bi are also derived from smelting Sn and Cu, for instance in Japan and China. However, in most cases Bi is a

significant smelter penalty; for example, a Bi content exceeding 500 ppm in a saleable copper concentrate incurs a penalty (George et al., 2018). Overall, there has been a move towards smelting cleaner concentrates, e.g. in China (Blazy and Hermant 2013; European Commission, 2017b; Krenev et al. 2015). Global Bi production is dominantly from Asia (Fig. 8), as indicated by annual production statistics (Brown et al., 2021).

Global production over the past decade had been dominated by China (Fig. 7), where Bi is a by-product of both Pb and W processing. However, production from the Masan Resources-owned Núi Pháo mine in Vietnam, rising from 646 t in 2014 to 3099 t in 2018 (Brown et al., 2020), fell to <1000 t in 2019 and 2020 (Brown et al., 2021; Masan Resources, 2020). The introduction of a new producer has changed market dynamics, and while production from Vietnam briefly surpassed that of China, it has now dropped to second place (Figs. 7 and 8). In China, artisanal mining for Bi also occurs, with manual separation of Bi-rich mineralisation contributing significantly to global production of concentrates (Blazy and Hermant 2013; European Commission, 2017b). However, few public data are available for artisanal Bi production and are not included in Figs. 7-9.

The longer-term (four-decade) trend in Bi production shows a consistent decrease until the late 1990s (Fig. 9). Market volatility in the mid-2000s affected production until the mid-2010s, and was followed by the sharpest sustained increase as production commenced at the Núi Pháo mine in Vietnam in 2014 (Fig. 9).

6.2. Bismuth processing and refining

High specific gravity, good flotability and diamagnetism of the most common Bi minerals enable the application of beneficiation methods involving flotation and gravity and magnetic separation (Krenev et al., 2015).

During the production of high purity Pb from primary sources, the Bi content of the concentrate determines the processing route taken. If the Bi content of lead concentrate is higher than 4%, the electrolytic route is preferred (Betts process). Bismuth is recovered from the impure mixture of metals left in the residual anode slimes. The slime is heated and Bi is finally recovered after a reduction step using carbon. If the Bi content is 0.05–3.5 %, the Kroll-Betterton process is preferred, which is based on the precipitation of Bi using Ca and Mg added to molten Pb (Blazy and Hermant 2013; European Commission, 2017b).

Recovery of Bi from Bi-bearing W and W-Mo ores is possible using a combination of gravity, flotation and magnetic separation, but it typically has low mean recovery of ~69 % (Krenev et al., 2015). In the processing of these ores, the majority of Bi is partitioned into the sulphide concentrate with the remainder separated into the W-Sn concentrate. The sulphide concentrate is processed by flotation, and Bi is removed from the W-Sn concentrate using magnetic separation, where the majority of the Bi follows the non-magnetic Sn stream, with a small amount following the magnetic W stream. Recovery of Bi from the sulphide stream uses a variety of Bi depressors, including cyanide, and ethyl xanthate as a collector. Cyanide-free technology for the recovery of Bi from some molybdenum flotation tails has been developed (Krenev et al., 2015). At Núi Pháo, the ore is separated into a Cu and Au stream and a bulk sulphide that contains W, Bi and F. The Bi is separated by further flotation and leaching from the bulk sulphide to form a Bi cement which is smelted into Bi ingots (Masan Resources, 2014a).

Limited information is available on the recovery of Bi from W ore in China. Ore from the Xihuashan W-bearing quartz vein deposit comprises scheelite, wolframite, cassiterite, bismuthinite, molybdenite, copper sulphides and some REE-bearing phases (Giuliani et al., 1988). Numerous flotation processing paths are undertaken to separate a bismuthinite concentrate, which is then sold on for further processing (Blazy and Hermant 2013; European Commission, 2017b).

Bismuth-bearing Cu ores are also possible feedstock for Bi production, since Bi tends to partition into the dust-gas phases (90%) and not into the waste slags (9.5%) (Krenev et al., 2015).

Ionometallurgy, using deep eutectic solvent (DES) ionic liquids, has been shown to dissolve Bi-bearing minerals such as tellurobismuthite (Bi_2Te_3) (Jenkin et al., 2016) from Au ore samples from Cononish gold mine, Scotland and Reed's Mine Georgia, United States. Hydrometallurgical and pyrometallurgical methods are typically energy intensive and generate significant amounts of carbon dioxide. In contrast, DES technology has the potential to reduce both environmental impacts and cost. Bismuth is often a waste product but there is potential for co-production, simultaneously adding value to the ore and removing potential environmental contaminants from the tailings (Jenkin et al., 2016). Thus, novel, selective, processing methods for Bi are possible.

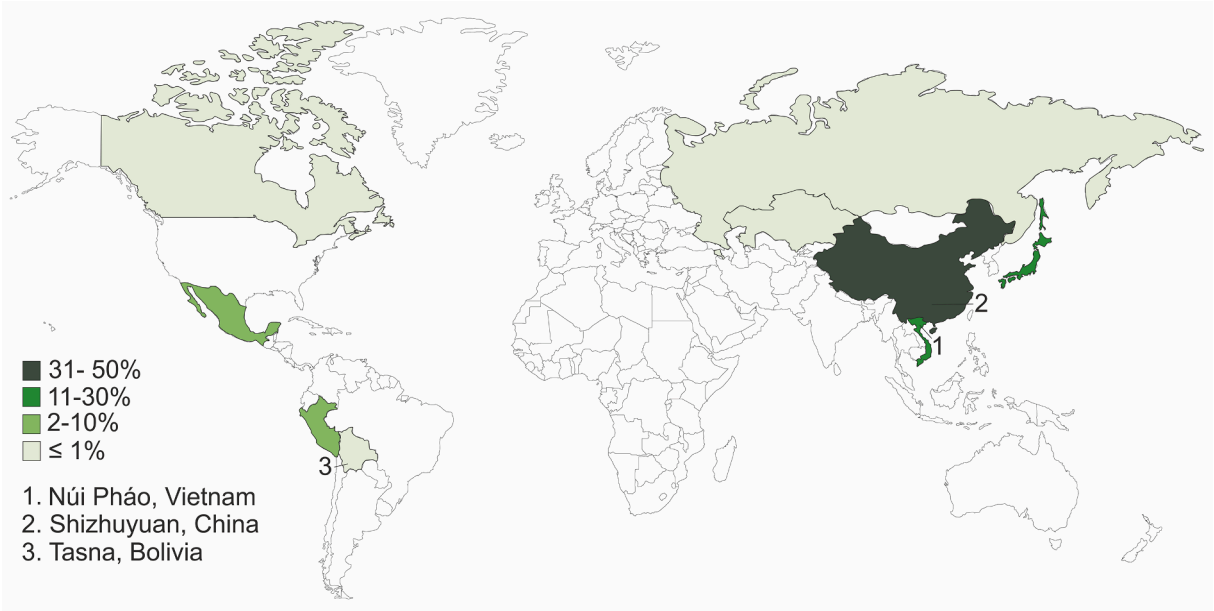

Fig. 8. The distribution of global Bi production in 2019 by market share. Data from the British Geological Survey (Brown et al., 2021), 2019 is the most recent year for which data exist.

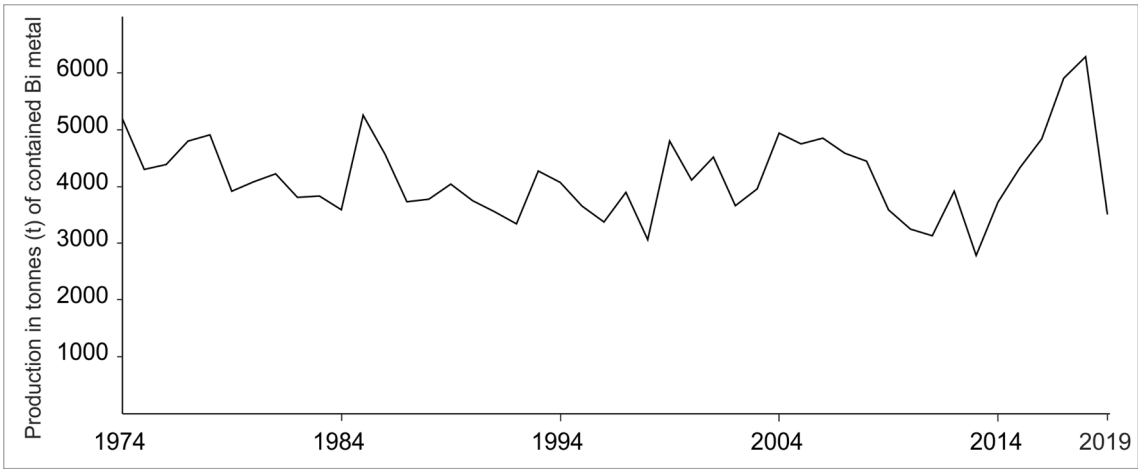

Fig. 9. Total annual Bi production (in tonnes of contained metal) from 1974 to 2019. Data from BGS World Mineral Statistics database (https://www.bgs.ac.uk/mineralsuk/statistics/worldStatistics.html).

6.3. Bismuth resources and reserves

Resource and reserve data for Bi are limited as Bi is not typically included in ore reserve calculations unless present in significant amounts. The limited data available are depicted in Fig. 10. The USGS does not publish Bi reserves due to the lack of quantitative data. World reserves of Bi are usually estimated from the Bi content of Pb resources because Bi production is most often a by-product of processing Pb ores (U.S. Geological Survey, 2021). The Núi Pháo mine in Vietnam published JORC-compliant proven and probable reserves of 66 Mt at 0.08% Bi, equating to approximately 53 000 t of Bi metal, and a measured, indicated and inferred resource of 96.5 Mt at 0.08% Bi in 2014 (Fig. 10) (Masan Resources, 2014b). The NICO deposit in northern Canada has published a NI 43-101-compliant proven and probable reserves of 33.1 Mt at 0.14 % Bi, equating to approximately 46 300 t of contained Bi metal (Fortune Minerals, 2014 (Micon International Ltd, 2014)). The Bi-bearing skarn deposit at Stormont has an inferred resource of 0.151 Mt at 0.17% Bi (Skirrow et al., 2013). Historic reserves at the Tasna mine (U.S. Geological Survey, 1994) are 700 000 t, grading 1.7% bismuth, 0.6% copper, 0.3% tin, and 1.5 g/t of gold. This was updated in 1996 to 500 000 t at 1.47% bismuth and 1.28% copper, with credits for gold, silver, and tungsten. Further Bi mineralisation was identified at the Tasna mine, in veins with grades of 3% Bi, 1.43% Cu, 0.2% W, and 4.21 g/t Au per ton (U.S. Geological Survey, 1996) but no tonnage data were presented. Plans by the former owners Corriente Resources, Inc. were to mine and process the ore at local smelters, which could have been converted from Zn to Bi-Cu production, thereby keeping metal production in country (U.S. Geological Survey, 1996). Unfortunately, insufficient funding and the low Bi price prevented recommencement of mining. Historic reserve estimates for bismuth from the Shizhuyuan Bi deposit in China (Zhong et al., 2017) and the San Francisco de los Andes Bi-bearing breccia deposit in Argentina (Testa et al., 2018) are also presented in Fig. 10.

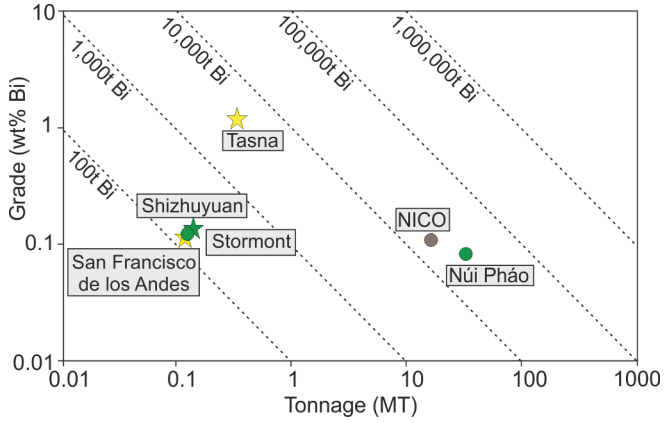

Fig. 10. The available Bi grade and tonnage of presented deposits. CRIRSCO-compliant total (proven and probable) reserve data are shown in circles (Núi Pháo, NICO); CRIRSCO-compliant resource data are shown as rectangles (Stormont) and historic reserves as stars (Tasna (U.S. Geological Survey, 1996), Shizhuyuan (Zhong et al., 2017) and San Francisco de los Andes (Testa et al., 2018)). Deposit types are coloured up according to the legend in Fig. 4.

6.4. Uses

Bismuth is not considered to be a human carcinogen (Kyle et al., 2011, Lambert, 1991, Slikkerveer and de Wolff, 1989) and is used in pharmaceuticals in the form of bismuth (III) nitrate ($Bi(NO_3)_3$) and bismuth subcarbonate ($(BiO)_2CO_3$). Bismuth subnitrate can be used in the treatment of gastrointestinal issues, while bismuth subcarbonate nanotubes have been synthesised and found to exhibit antibacterial properties against *Helicobacter pylori*, the bacteria that causes stomach ulcers (Chen et al., 2006). Bismuth subsalicylate is used as a treatment for stomach upset as the medicine “Pepto-Bismol”. In cosmetic applications the pigment bismuth oxychloride (BiClO) gives a pearlescent sheen to make-up (Völz et al., 2006).

Bismuth is used as a non-toxic, environmentally-friendly substitute for lead in alloys, being especially useful in water pipes and meters, hunting ammunition, fishing equipment and in paint (Block, 2005). The Safe Drinking Water Act Amendment of 1996 in the United States, which required that all new and repaired fixtures and pipes for potable water supply be lead free after August 1998, opened a wider market for bismuth as a metallurgical additive to lead-free pipe fittings, fixtures and water meters (U.S. Geological Survey, 2018). Bismuth alloys with tin and cadmium are used in triggering devices for fire detectors and extinguishers. These alloys are also used to manufacture holding devices for grinding optical lenses and turbine blades. Bismuth telluride is another important bismuth alloy due to its thermoelectric properties, which allow it to be used in thermal electricity generations (Satterthwaite and Ure, 1957). More machinable Bi-Zn alloys have been developed for the galvanisation process (U.S. Geological Survey, 2013). Lead-free plasma TVs and plasma displays also incorporate bismuth, where bismuth oxide substitutes for lead oxide in glass (Tarafder et al., 2010).

Bi–Pb eutectic compositions are effective heavy liquid coolants for nuclear reactors, and several recent reactor prototypes use steam generation modules in direct contact with the liquid metal coolant (Gorse-

Pomonti and Russier, 2007, Terlain et al., 2007, Tooth et al., 2013). The lead-bismuth eutectic (LBE) alloy (44.5 wt% Pb, 55.5 wt% Bi) is considered a potential candidate for the "*coolant of new generation fast reactors (critical and subcritical) and for liquid spallation neutron sources and accelerated driven systems (ADS).*" (Sobolev and Benamati, 2007). Another potential new use for Bi in energy generation is the solar generation of hydrogen fuel. Bismuth vanadate has been identified as a key component in the sunlight-mediated dissociation of water into hydrogen and oxygen, and reduces energy requirements by 8% (Kim et al., 2015, U.S. Geological Survey, 2017).

Constant development of new uses for Bi and Bi compounds include semiconductors (Jain et al., 2019, Wu et al., 2019) and as microbial agents (Wang et al., 2018). While technologies are not yet ready for commercial production, they have the future potential to drive demand for Bi.

6.5. Demand

Global demand for Bi is forecast to grow at 4–5% per year, due mainly to increasing demand in pharmaceutical applications (European Commission, 2017b). Although there are many metallurgical applications currently available, and many more being researched, this accounts for only one third of annual demand with the remainder used in Bi chemicals production. The forecast increase is also driven by industrial demand in emerging economies and Bi being used as a replacement for Pb. International agreements to eliminate lead from solder in manufacturing processes by 2005 in Europe, Japan, and North America resulted in increased consumption of Bi as an appropriate substitute (JEITA, 2002).

6.6. Price and trade

The price of bismuth, typically reported for bismuth metal with 99.99% Bi minimum, has fluctuated significantly over the past decade, which has had direct impacts on demand. China reorganised and concentrated its Bi production in 2007; numerous smelters closed and Bi output was reduced. As a consequence of this supply bottle neck, the price of Bi rose dramatically to over US$40/kg. Shortly afterwards, prices dropped to US$15/kg (2007–2008) during the financial crisis and, despite some speculative purchasing which briefly raised prices, it dropped to around US$10/kg in 2015. Although prices remained stable until 2017 (European Commission, 2017b), there has been a subsequent significant decline to a 25-year low of US$5.50/kg in 2019 (Fig. 11) (5N Plus, 2019).

2019 is regarded as one of the poorest years for bismuth prices; they dropped by 27% and ended the year almost 40% lower than in 2015, previously viewed as one of the poorest years (5N Plus, 2019). Price drops were in part driven by trade disputes between the US and China. The US introduced a 10% import tariff on Chinese bismuth products in September 2018 and increased it to 25% in May 2019. This forced suppliers to cut their offer prices during the first half of 2019 to stimulate export demand. The price decrease may also be due to the ramping up of production at Núi Pháo in Vietnam, with significant increases in total bismuth production since 2014 (Figs. 8 and 9).

The EU was 100% reliant on imports of refined bismuth metal between 2010 and 2014, with 84% of all imports sourced from China (European Commission, 2017b). The 5N Plus facility in Germany accounts for 94% of all Bi imports into the 27 countries in the European Union (EU-27) (1488 t in 2019). The market share of reported imports of bismuth '*articles including waste and scrap*' (UN trade code 810600) into Germany has changed dramatically over the period 2017 to 2019. In 2017, China supplied ~70% of Bi imports and 28% came from EU-27. In 2018 the market share of imports from China dropped by almost 30% to 41% while EU-27 imports remained approximately the same at ~32%. The remainder was covered by a new trade flow of imports from Lao - People's Democratic Republic, with a market share of 24%. This grew to a market share of 55% in 2019, reducing Chinese import of Bi into Germany to 30% and EU-27 market share to 12% (data source: DESA/UNSD, United Nations Comtrade database). Although unconfirmed, it is presumed that this source of Bi is from the Núi Pháo mine in Vietnam.

6.7. Recycling and substitution

The rate of recovery of Bi from end-of-life products is under 1% (European Commission, 2020b, Graedel et al., 2011). Its use in dissipative applications such as pigments and pharmaceuticals mean it is very difficult to recover and recycle. The most likely candidates for recycling are solder alloys, typically found in electronic equipment. Recycled Bi-Sn alloy has been tested as an improver of the machining properties of lead-free brass and offers a possibility for new and better lead-free brass alloys (Suksongkarm et al., 2017). Hydrometallurgical recovery of Bi from copper smelter converter dust has been trialled as a potential secondary source of Bi. Up to 92% recovery efficacy was achieved using a two-acid digest leaching of Bi from converter dust, producing a potentially commercially viable product of Bi_2O_3 at 97.8% (Ha et al., 2015).

Limited substitutions for Bi in pharmaceutical applications include alumina and magnesia. Lead, Se and Te are Bi substitutions in free-machining alloys, while In can replace Bi in low-temperature solders (U.S. Geological Survey, 2020). The European Commission lists a

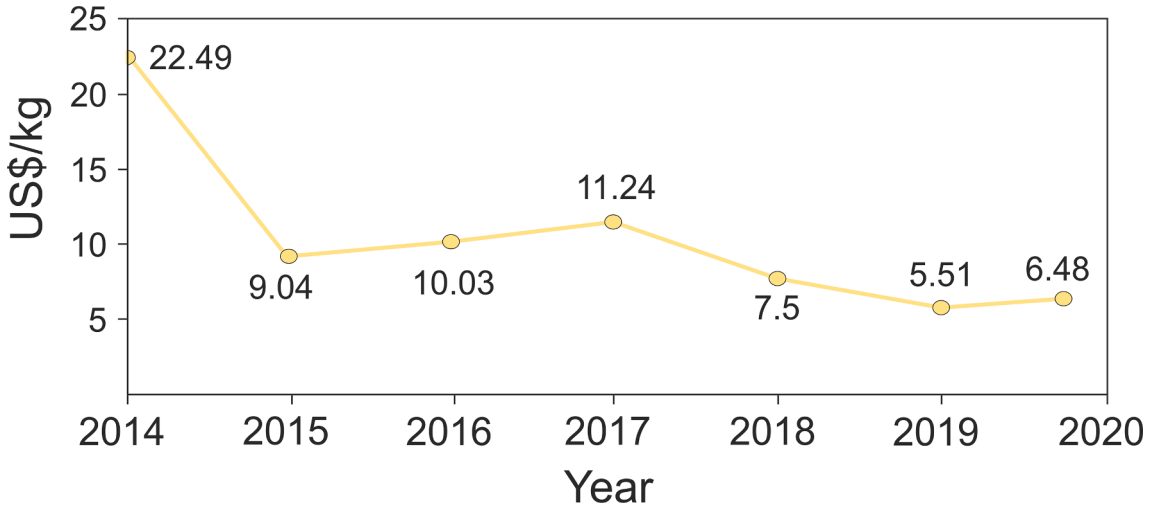

Fig. 11. Bismuth price in US$/kg, 2014–2020 (September 2020 data available only) (5N Plus, 2019).

substitution index of 0.96 and 0.94 (calculated substitution index (SI) for economic importance (EI) and supply risk (SR) indices respectively) out of a maximum of 1.0, indicating that overall limited substitution for Bi occurs in practice (European Commission, 2020b).

7. Discussion

The medically safe, energy-related and modern non-toxic alloying applications of Bi demonstrate its economic importance, and the concentration of production in Asia suggests there is risk of supply disruption. Its high ranking in these criticality assessment indices has resulted in it being classified as 'critical' by the EU, the USA, Australia and the UK (British Geological Survey, 2015; Commonwealth of Australia, 2020; European Commission, 2020a; U.S. Department of the Interior, 2018). Despite its critical status, it suffers from industrial inertia, whereby it is judged perhaps too costly or complex to extract as a by-product and therefore is regarded as deleterious. Although Bi is primarily extracted as a by-product from the processing of ore from W and Pb deposits, and production is highly concentrated in a few countries, we have outlined the wide range of deposit types within which bismuth occurs.

This contribution has highlighted the principal occurrences of, uses for, and issues surrounding the production of, bismuth. We also recommend three intervention points that may result in lessening perceived criticality, and thereby reducing volatility (Renner and Wellmer, 2019), of the bismuth market: 1) the inclusion of minor metals in initial assay reporting of exploration samples; 2) the uptake of improved resource and reserve reporting approaches; and 3) an appreciation of the deportment and tenor of bismuth, and other minor metals, in designing processing flow sheets.

7.1. Intervention points

The knowledge base for bismuth can be improved upon through interventions at the exploration, resource and reserve reporting and mineral processing planning stages. However, this requires a change in mindset regarding metals traditionally viewed as deleterious or waste. Continuing to ignore the presence of minor metals risks underestimation of their availability, further enhancing critical status. As such, the global abundance of Bi within economic deposits may be greater than is currently apparent.

Bismuth has long been used as a pathfinder element, along with Sb, As, and Hg, during gold mineralisation. Although a valid practice, such use has created a reporting bias, whereby the gold, and other valuable elements, are reported while minor metals such as Bi are disregarded as geochemical anomalies. In other deposit types, where Bi mineralisation might be encountered, such as skarn, W-Sn granite-greisen and reduced intrusion-related Au-Bi deposits, Bi should be included in a representative subset of sample assays so that by-product potential is not overlooked. Following on from this, supporting mineralogical analysis of samples should be made to identify Bi deportment within all ore and gangue minerals. The cost of additional geochemical and petrographic analysis may be outweighed by the possible increased revenues from minor metal by-production. At the very least, it contributes to a better overall understanding of the deportment of metals and therefore the metallurgy of the ore body.

Under-reporting of minor metals is endemic in exploration. The assessment and release of the maiden compliant resource estimate is a key stage for fund-raising and gaining recognition for all exploration projects. The responsibility to assess all potential economic metals in the deposit lies with the exploration company. However, top down support for the inclusion of resources estimates for minor metals from CRIRSCO (Committee for Mineral Reserves International Reporting Standards) could result in a significant increase in our knowledge base for the potential resources and reserves of minor metals and as such reduce the volatility in those markets. The use of other reporting methodologies such as the UNFC (United Nations Framework Classification for Resources) allows for the inclusion of other types of estimate (undiscovered, uneconomic, or unrecoverable minerals) that are not covered by CRIRSCO standards (UN Economic and Social Council, 2014), which may be the case for some minor metals such as Bi. Where data would not typically be recorded or held consistently (if at all) by minerals companies, even when they may use them for their own planning purposes, the UNFC methodology allows these other estimates to be recorded.

Mineralogical evaluation during the early stages of exploration means appropriate processing strategies can be incorporated into feasibility studies. The geometallurgical information garnered early on in a project allows for the development of processing flow sheets preventing unforeseen complications with the final processing work flow. For example, Bi content between 200 and 500 ppm in copper concentrate incurs a smelter penalty (George et al., 2018). Understanding the metallurgical characteristics of the ore when designing mineral processing flowsheets reduces the risk of inefficiency and waste. In this way exploration and mining companies can create maximum value for initial assay and mineralogical reporting through the optimisation of the integration of mining and mineral processing.

These interventions have the added benefit of supporting the extractives industry to take a more sustainable approach to mining. If the global mining community is to achieve more responsible production, using the UN sustainable development goals, e.g. No. 12 'Responsible Consumption and Production' and No. 8 'Decent Work and Economic Growth', as a blueprint for example, then it is important that the full metal budget of the deposit is taken into consideration. Furthermore, while Bi is not a human carcinogen (Kyle et al. 2011; Lambert 1991; Slikkerveer and de Wolff 1989), and more generally considered a non-toxic element, the environmental risks associated with the presence of heavy metals in waste material in tailing dams are another factor to be considered when evaluating whether or not a metal should be extracted from a particular ore.

7.2. A geological model for bismuth

Bismuth occurs in a variety of crustal mineral deposit types (section 5) in association with a range of major commodities (Pb, Au, W) but there is no unified geological model for Bi mineralisation. Tracking the distribution of Bi across the geological cycle can help recognise sources, sinks, pathways and traps for Bi mineralisation thereby improving baseline knowledge for Bi exploration. Here we present a broad geomodel for Bi, highlighting the main pathways for Bi cycling in the Earth's crust.

Bismuth occurs in upper oceanic crust, hosted in volcanic glass, and so can be released from the subducting slab into the mantle wedge above a subduction zone (Jenner, 2017). The implication is that the majority of Bi host-phases in the upper oceanic crust are unstable during subduction, permitting their mobilisation by slab-derived fluids. Potential hosts of Bi include low-temperature hydrothermal sulphides, sulphosalts and serpentine minerals (Jenner, 2017).

Relatively little literature exists on the magmatic geochemistry of bismuth, however, the partition coefficients for Bi in clinopyroxene and garnet in basanite (Adam and Green, 2006) indicate incompatible behaviour of these elements during melting. Further evidence for the incompatible nature of Bi in melt comes from the Variscan granites of south west England where Bi is enriched in the feldspar-dominated assemblage of the G2, G3 and G4 granites (Simons et al., 2017). Thus, Bi will tend to be concentrated in the most evolved magmas in collisional to post-collisional settings, and may be partitioned into late-magmatic fluids.

Bismuth behaviour in hydrothermal systems is better understood, in part due to the role of low temperature (271 °C) Bi melt as a collector for gold in magmatic-hydrothermal systems. The mobility of Bi in hydrothermal systems drives its ubiquity in magmatic-hydrothermal deposit types. The presence or absence of Pb in the hydrothermal system is a key controlling mechanism in the deportment of Bi minerals. In high-Pb,

high sulphidation systems, Bi is incorporated isomorphously into galena, resulting in Bi-rich galena, a key ore mineral for Bi. In high sulphidation, low Pb systems, Bi partitions into chalcopyrite (George et al., 2016; George et al., 2018) and the sulphide bismuthinite. In systems where chalcopyrite is absent but bornite and/or chalcocite are present, such as Olympic Dam, Australia, these minerals are likely to host, and control the distribution of Ag and Bi (Cook et al., 2015).

It has been proposed that the redistribution of Bi back to the ocean is dominated by aeolian processes where particulate Bi is reworked from arid land masses (Bertine et al., 1996). Subsequent uptake by marine algae (up to 140 ppm in non-calcareous red algae), along with the reactivity of Bi complexes in particular with Mn complexes, results in lower levels of Bi below 500 m depth of water column compared to water <500 m depth. The Bi content of shallow water manganese nodules is up to 22 ppm (Bertine et al., 1996). Where there is variation in Bi content of global subduction-zone magmas, this is likely due to an overprinting by a sediment component in the melt (Jenner, 2017). Subducting ferromanganese crusts and pelagic clay lithologies (up to 1600 ppb) (Bertine et al., 1996) and black shales that can contain Bi up to several hundred ppm (Lipinski et al., 2003) are potential sedimentary sources of source of Bi in subduction zones.

7.3. Benefits of a comprehensive geological model for bismuth

A geological model centred on bismuth (rather than it being a collector or pathfinder element) and focussing on bismuth behaviour in magmatic systems would aid in tracing Bi through the geological cycle. At a crustal scale, a deeper appreciation of the physico-chemical aspects of bismuth behaviour in different deposit types, in particular those that are not gold rich, would help define the location and probable mineralogy of bismuth within ore deposits. This in turn would lead to focussed exploration campaigns whereby specific deposit type(s) could be targeted, with an understanding of the important mineral phases, and where potential mineralisation may occur. Knowledge garnered from the improved reporting of Bi content in assays, and petrographic descriptions from exploration projects would significantly increase the available data to help build a geomodel appropriate to all deposit types.

In the context of gold mineralisation, the behaviour of bismuth in geological and surface environments is key because bismuth is important as a pathfinder element for gold and because molten bismuth collects gold in hydrothermal systems. The development of the bismuth collector model (section 4.2) (Ciobanu et al., 2006a; Ciobanu et al. 2005; Douglas et al., 2000; Tooth et al. 2008; Tooth et al. 2011) demonstrates the importance of bismuth and bismuth-related melts in increasing the gold content of deposits, and more generally in understanding ore metallogenesis. However, there has been selective consideration of Bi as collector because it was seen as a pathfinder for gold. Little information is available on the impact of changing efficiency of Bi collection on other modern tech metals, for example tellurium.

Improved analytical inclusion and reporting of Bi content would aid further petrogenetic research. The mineral chemistry and paragenesis of Bi-bearing minerals can be used to characterise the behaviour of fluids in the formation of pegmatites for example, despite being a volumetrically negligible part of the whole pegmatite body (Škoda et al., 2021). This highlights how minor metals can enhance our understanding of the processes and mechanisms of deposit formation.

There is a paucity of whole-rock analyses that include Bi. Chiaradia (2020) proposes a higher efficiency of Au precipitation in alkaline systems than in the Cu-rich calc-alkaline systems, using Cu and Au data for analysis. An additional factor that should be considered in these simulations is the Bi content. Its ability to scavenge and carry gold down to ppb level in magmatic-hydrothermal fluids could be a part of the controlling mechanism and so should be considered in experimental modelling of precipitation. The lack of available Bi data precludes the testing of the hypothesis outlined above. This dearth of data additionally weakens attempts at better understanding the bismuth life cycles, both geological and anthropogenic.

8. Conclusions

1. Bismuth occurs in a wide range of mineral deposit types, signifying that the geological availability of Bi is not the major factor in the security of supply of bismuth. The perceived criticality of bismuth is due to its market concentration and the recognition that it has many valuable end-uses, with a high proportion in dissipative products that are not recoverable. The supply bottlenecks are primarily due to the concentration of production to a few countries, and to an extent, the industrial inertia that has led to Bi being disregarded as a valuable by-product.
2. A changing attitude towards minor metals within the mining industry would result in an overall increased understanding of mineralisation and genetic models of geological systems, with more research and development of models for Bi mineralisation. Its use as a pathfinder element, and the recent elucidation of the Bi collector model for gold, highlights its importance in understanding big scale geological processes. To meet the challenges of the future, exploration and resource reporting has an important role to play in informing the entire supply chain. A holistic approach by the mining industry to the entire metal budget of projects can potentially alleviate global concerns over supply chain disruption.

Declaration of Competing Interest

The authors declare that they have no known competing financial interests or personal relationships that could have appeared to influence the work reported in this paper.

Acknowledgements

The authors would like to thank Gus Gunn (BGS) for a thorough and constructive internal review and the reviewer Haoyang Zhou (University of Oslo) whose constructive criticism strengthened this contribution. ED and KG publish with the permission of the Director of the British Geological Survey ©UKRI 2022.

Appendix A. Supplementary data

Supplementary data to this article can be found online at https://doi.org/10.1016/j.oregeorev.2022.104722.

References

5N Plus. 2019. 2019 Annual Report.
Acosta-Góngora, P., Gleeson, S., Samson, I., Corriveau, L., Ootes, L., Taylor, B., et al., 2015a. Genesis of the Paleoproterozoic NICO iron oxide–cobalt–gold–bismuth deposit, Northwest Territories, Canada: Evidence from isotope geochemistry and fluid inclusions. Precambrian Research. 268, 168–193.
Acosta-Góngora, P., Gleeson, S., Samson, I., Ootes, L., Corriveau, L., 2014. Trace element geochemistry of magnetite and its relationship to Cu-Bi-Co-Au-Ag-UW mineralization in the Great Bear magmatic zone, NWT. Canada. Economic Geology. 109, 1901–1928.
Acosta-Góngora, P., Gleeson, S., Samson, I., Ootes, L., Corriveau, L., 2015b. Gold refining by bismuth melts in the iron oxide-dominated NICO Au-Co-Bi (±Cu±W) deposit, NWT. Canada. Economic Geology. 110, 291–314.
Adam, J., Green, T., 2006. Trace element partitioning between mica-and amphibole-bearing garnet lherzolite and hydrous basanitic melt: 1. Experimental results and the investigation of controls on partitioning behaviour. Contributions to Mineralogy and Petrology. 152, 1–17.
Afifi, A.M., Kelly, W.C., Essene, E.J., 1988a. Phase relations among tellurides, sulfides, and oxides; I, Thermochemical data and calculated equilibria. Economic Geology. 83, 377–394.
Afifi, A.M., Kelly, W.C., Essene, E.J., 1988b. Phase relations among tellurides, sulfides, and oxides; Pt. II, Applications to telluride-bearing ore deposits. Economic Geology. 83, 395–404.
Angino, EE., 1979. Bismuth: Element and Geochemistry. In: Angino, E.E., Long, D.T. (Eds.), Geochemistry of Bismuth. Dowden Hutchinson and Ross.
Badanina, E.V., Trumbull, R.B., Dulski, P., Wiedenbeck, M., Veksler, I.V., Syritso, L.F., 2006. The behavior of rare-earth and lithophile trace elements in rare-metal

granites: a study of fluorite, melt inclusions and host rocks from the Khangilay complex, Transbaikalia. Russia. The Canadian Mineralogist. 44, 667–692.
Baker, T., Pollard, P., Mustard, R., Mark, G., Graham, J., 2005. A comparison of granite-related Sn, W, and Au-Bi deposits: implications for exploration. SGA Newsletter. 61, 10–17.
Baldwin, J., Hill, P., Finch, A., Von Knorring, O., Oliver, G., 2005. Microlite-manganotantalite exsolution lamellae: evidence from rare-metal pegmatite, Karibib. Namibia. Mineralogical Magazine. 69, 917–935.
Ball, T., Basham, I., 1984. Petrogenesis of the Bosworgey granitic cusp in the SW England tin province and its implications for ore mineral genesis. Mineralium Deposita. 19, 70–77.
Ball T, Basham I, Blank D, Smith T. Aspects of the geochemistry of bismuth in South-West England. Proceedings of the Ussher Society. 1982;5:376-82.
Bandy, M.C., 1951. The Ribaue-Alto Ligonha Pegmatite District, Portuguese East Africa. Rocks & Minerals. 26, 512–521.
Belogub, E., Moloshag, V., Novoselov, K., Kotlyarov, V., 2011. Native bismuth, tsumoite, and Pb-bearing tsumoite from the Tarn'er copper-zinc massive sulfide deposit, northern Urals. Geology of Ore Deposits. 53, 798–805.
Benninger, L.M., Koski, R.A., 1987. Descriptions and chemical analyses of sulfide samples dredged in 1986 from Escanaba Trough, southern Gorda Ridge. US Geological Survey.
Berkenbosch, H., De Ronde, C., Gemmell, J., McNeill, A., Goemann, K., 2012. Mineralogy and formation of black smoker chimneys from Brothers submarine volcano. Kermadec arc. Economic Geology. 107, 1613–1633.
Bertine, K.K., Koide, M., Goldberg, E.D., 1996. Comparative marine chemistries of some trivalent metals—bismuth, rhodium and rare earth elements. Marine Chemistry. 53, 89–100.
Bespaev, H., Globa, V., Abishev, V., Gulyaeve, N., 1996. Gold fields of Kazakhstan. Mineral Resources of Kazakhstan, Committee for Geology and Underground Resources Protection and Use of the Ministry of Energy and Natural Resources of the Replublic of. Kazakhstan. 75–76.
Bettencourt, J.S., Juliani, C., Xavier, R.P., Monteiro, L.V., Neto, A.C.B., Klein, E.L., et al., 2016. Metallogenetic systems associated with granitoid magmatism in the Amazonian Craton: An overview of the present level of understanding and exploration significance. Journal of South American Earth Sciences. 68, 22–49.
Blazy P, Hermant V. Métallurgie extractive du bismuth. Éditions Techniques de l'Ingénieur, doc. M 2316, pp.152013.
Block L. Where Lead Lies. In: University of North Carolina, editor. Lead Poisoning Prevention Program 2005.
Breiter, K., Förster, H.-J., Škoda, R., 2006. Extreme P-, Bi-, Nb-, Sc-, U-and F-rich zircon from fractionated perphosphorous granites: The peraluminous Podlesí granite system. Czech Republic. Lithos. 88, 15–34.
British Geological Survey, 2011. Risk list 2011.
British Geological Survey, 2012. Risk list 2012.
British Geological Survey, 2015. Risk list 2015.
Brookins, D.G., 1988. Bismuth. Springer, Eh-pH Diagrams for Geochemistry, pp. 32–33.
Brown, T.J., Idoine, N.E., Wrighton, C.E., Raycraft, E.R., Hobbs, S.F., Shaw, R.A., Everett, P., Deady, E.A., Kresse, C., 2021. World Mineral Production 2015-19. British Geological Survey, Keyworth, Nottingham.
Brown, T.J., Idoine, N.E., Wrighton, C.E., Raycraft, E.R., Hobbs, S.F., Shaw, R.A., Everett, P., Kresse, C., Deady, E.A., Bide, T., 2020. World Mineral Production 2014-18. British Geological Survey, Keyworth, Nottingham.
Brugger, J., Liu, W., Etschmann, B., Mei, Y., Sherman, D.M., Testemale, D., 2016. A review of the coordination chemistry of hydrothermal systems, or do coordination changes make ore deposits? Chemical Geology. 447, 219–253.
Burisch, M., Gerdes, A., Walter, B.F., Neumann, U., Fettel, M., Markl, G., 2017. Methane and the origin of five-element veins: mineralogy, age, fluid inclusion chemistry and ore forming processes in the Odenwald. SW Germany. Ore Geology Reviews. 81, 42–61.
Buzatu, A., Damian, G., Dill, H.G., Buzgar, N., Apopei, A.I., 2015. Mineralogy and geochemistry of sulfosalts from Baia Sprie ore deposit (Romania) — New bismuth minerals occurrence. Ore Geology Reviews. 65, 132–147.
Cabral, A.R., Ließmann, W., Jian, W., Lehmann, B., 2017. Bismuth selenides from St. Andreasberg, Germany: an oxidised five-element style of mineralisation and its relation to post-Variscan vein-type deposits of central Europe. International Journal of Earth Sciences. 106, 2359–2369.
Carlin J, JF. Bismuth. In: U.S. Bureau of Mines, editor. Mineral Facts and Problems 1985.
Cepedal, A., Fuertes-Fuente, M., Martin-Izard, A., Gonzalez-Nistal, S., Rodriguez-Pevida, L., 2006. Tellurides, selenides and Bi-mineral assemblages from the Río Narcea Gold Belt, Asturias, Spain: genetic implications in Cu–Au and Au skarns. Mineralogy and Petrology. 87, 277–304.
Chapman, R., Allan, M., Mortensen, J., Wrighton, T., Grimshaw, M., 2018. A new indicator mineral methodology based on a generic Bi-Pb-Te-S mineral inclusion signature in detrital gold from porphyry and low/intermediate sulfidation epithermal environments in Yukon Territory. Canada. Mineralium Deposita. 53, 815–834.
Chen, R., So, M.H., Yang, J., Deng, F., Che, C.-M., Sun, H., 2006. Fabrication of bismuth subcarbonate nanotube arrays from bismuth citrate. Chemical Communications. 2265–7.
Chiaradia, M., 2020. Gold endowments of porphyry deposits controlled by precipitation efficiency. Nature communications. 11, 1–10.
Christy, A.G., 2015. Causes of anomalous mineralogical diversity in the Periodic Table. Mineralogical Magazine. 79, 33–50.
Ciobanu, C., Cook, N., Damian, F., Damian, G., 2006a. Gold scavenged by bismuth melts: An example from Alpine shear-remobilizates in the Highiş Massif. Romania. Mineralogy and Petrology. 87, 351–384.
Ciobanu, C.L., Birch, W.D., Cook, N.J., Pring, A., Grundler, P.V., 2010. Petrogenetic significance of Au–Bi–Te–S associations: the example of Maldon, Central Victorian gold province. Australia. Lithos. 116, 1–17.
Ciobanu, C.L., Cook, N.J., 2000. Intergrowths of bismuth sulphosalts from the Ocna de Fier Fe-skarn deposit, Banat. Southwest Romania. European Journal of Mineralogy. 12, 899–917.
Ciobanu, C.L., Cook, N.J., 2004. Skarn textures and a case study: the Ocna de Fier-Dognecea orefield, Banat. Romania. Ore Geology Reviews. 24, 315–370.
Ciobanu, C.L., Cook, N.J., Pring, A., 2005. Bismuth tellurides as gold scavengers. In: Mineral deposit research: Meeting the global challenge: Springer, pp. 1383–1386.
Ciobanu, C.L., Cook, N.J., Pring, A., Brugger, J., Danyushevsky, L.V., Shimizu, M., 2009. 'Invisible gold'in bismuth chalcogenides. Geochimica et Cosmochimica Acta. 73, 1970–1999.
Ciobanu CL, Cook NJ, Spry PG. Preface-Special Issue: Telluride and selenide minerals in gold deposits-how and why? Mineralogy and Petrology. 2006b;87:163.
Ciobanu, C.L., Cook, N.J., Stein, H., 2002. Regional setting and geochronology of the Late Cretaceous Banatitic magmatic and metallogenetic belt. Mineralium Deposita. 37, 541–567.
Cockerton, A.B., Tomkins, A.G., 2012. Insights into the liquid bismuth collector model through analysis of the Bi-Au Stormont skarn prospect, northwest Tasmania. Economic Geology. 107, 667–682.
Commonwealth of Australia, 2020. Australian Critical Metals Prospectus 2020.
Cook, N., Ciobanu, C., 2001. Paragenesis of Cu-Fe ores from Ocna de Fier-Dognecea (Romania), typifying fluid plume mineralization in a proximal skarn setting. Mineralogical Magazine. 65, 351–372.
Cook, N., Ciobanu, C., 2004. Bismuth tellurides and sulphosalts from the Larga hydrothermal system, Metaliferi Mts, Romania: Paragenesis and genetic significance. Mineralogical Magazine. 68, 301–321.
Cook, N.J., Ciobanu, C., Danyushevsky, L., Gilbert, S., 2011. Minor and trace elements in bornite and associated Cu–(Fe)-sulfides: A LA-ICP-MS study Bornite mineral chemistry. Geochimica et Cosmochimica Acta. 75, 6473–6496.
Cook NJ, Ciobanu CL, Ehrig K. Insights into zonation within the Olympic Dam Cu-U-Au-Ag deposit from trace element signatures of sulfide minerals. Abstract, SEG 2015 Conference, Hobart, Tasmania, Australia 2015.
Cook, N.J., Ciobanu, C.L., Stanley, C.J., Paar, W.H., Sundblad, K., 2007a. Compositional data for Bi–Pb tellurosulfides. The Canadian Mineralogist. 45, 417–435.
Cook, N.J., Ciobanu, C.L., Wagner, T., Stanley, C.J., 2007b. Minerals of the system Bi–Te–Se–S related to the tetradymite archetype: review of classification and compositional variation. The Canadian Mineralogist. 45, 665–708.
Damian, G., Ciobanu, C.L., Cook, N.J., Damian, F., 2008. Bismuth sulphosalts from the galena-matildite series in the Cremenea vein, Şuior, Baia Mare district, Romania. Neues Jahrbuch für Mineralogie-Abhandlungen: Journal of Mineralogy and Geochemistry. 185, 199–213.
Davis, W., Williams-Jones, A., 1985. A fluid inclusion study of the porphyry-greisen, tungsten-molybdenum deposit at Mount Pleasant, New Brunswick. Canada. Mineralium Deposita. 20, 94–101.
De Caritat, P., Cooper, M., 2016. A continental-scale geochemical atlas for resource exploration and environmental management: the National Geochemical Survey of Australia. Geochemistry: Exploration, Environment, Analysis. 16, 3–13.
de la Campa, A.M.S., Jesus, D., Fernández-Caliani, J.C., González-Castanedo, Y., 2011. Impact of abandoned mine waste on atmospheric respirable particulate matter in the historic mining district of Río Tinto (Iberian Pyrite Belt). Environmental research. 111, 1018–1023.
de Ronde, C.E., Massoth, G.J., Butterfield, D.A., Christenson, B.W., Ishibashi, J., Ditchburn, R.G., et al., 2011. Submarine hydrothermal activity and gold-rich mineralization at Brothers Volcano, Kermadec Arc. New Zealand. Mineralium Deposita. 46, 541–584.
Dekov, V.M., Savelli, C., 2004. Hydrothermal activity in the SE Tyrrhenian Sea: an overview of 30 years of research. Marine Geology. 204, 161–185.
Dimitrova, D., Kerestedjian, T., 2006. Bismuth minerals in the postskarn sulphide-arsenide mineralization in the Martinovo iron deposit, NW Bulgaria. Geochem Mineral Petrol (Sofia). 44, 19–32.
Dini, A., Orlandi, P., 2010. A new gold-bismuth occurrence at Punta del Fenaio (Giglio Island, Tuscany). Atti Soc tosc Sci nat, Mem, Serie A. 115, 73–82.
Dobbe, R., 1991. Tellurides, selenides and associated minerals in the Tunaberg copper deposits, SE Bergslagen. Central Sweden. Mineralogy and Petrology. 44, 89–106.
Douglas, N., Mavrogenes, J., Hack, A., England, R., 2000. The liquid bismuth collector model: an alternative gold deposition mechanism. Geological Society of Australia Abstracts. Geological Society of Australia 1999, 135.
Dziggel, A., Wulff, K., Kolb, J., Meyer, F., 2009. Processes of high-T fluid–rock interaction during gold mineralization in carbonate-bearing metasediments: the Navachab gold deposit. Namibia. Mineralium Deposita. 44, 665–687.
Elliott, J.E., Kamilli, R.J., Miller, W.R., Livo, K.E., 1995. Vein and greisen Sn and W deposits. Preliminary compilation of descriptive geoenvironemental mineral deposits models United States Geological Survey. Denver. 62–69.
Eremin, N., Sergeeva, N., Dergachev, A., 2007. Rare minerals from massive sulfide ores: Typomorphic features and geochemical trend. Moscow University Geology Bulletin. 62, 98–106.
Etschmann, B.E., Liu, W., Pring, A., Grundler, P.V., Tooth, B., Borg, S., et al., 2016. The role of Te (IV) and Bi (III) chloride complexes in hydrothermal mass transfer: An X-ray absorption spectroscopic study. Chemical Geology. 425, 37–51.
European Commission. Communication from the Commission to the European Parliment, the Council, the European Economic and Social Committee and the Committee of the Regions on the 2017 list of Critical Raw Materials for the EU COM/2017/0490 final. 2017a.

European Commission. Study on the review of the list of critical raw materials. Critical raw materials factsheets. 2017b.
European Commission. Communication from the Commission to the European Parliment, the Council, the European Economic and Social Committee and the Committee of the Regions Critical Raw Materials Resilience: Charting a Path towards greater Security and Sustainability. COM/2020/474 final. 2020a.
European Commission. Study on the EU's list of Critical Raw Materials – Final Report (2020). 2020b.
Foord EE. Clinobisvanite, eulytite, and namibite from the Pala pegmatite district, San Diego Co., California, USA. Mineralogical Magazine. 1996;60:387-8.
Foord, E.E., Shawe, D., Conklin, N.M., 1988. Coexisting galena, PbS and sulfosalts: Evidence for multiple episodes of mineralization in the Round Mountain and Manhattan gold districts. Nevada. Canadian Mineralogist. 26, 355–376.
Fuertes-Fuente, M., Cepedal, A., Lima, A., Doria, A., dos Anjos, R.M., Guedes, A., 2016. The Au-bearing vein system of the Limarinho deposit (northern Portugal): Genetic constraints from Bi-chalcogenides and Bi–Pb–Ag sulfosalts, fluid inclusions and stable isotopes. Ore Geology Reviews. 72, 213–231.
Galliski MÁ. Distrito minero El Quemado, Deptos. La Poma y Cachi, provincia de Salta. II. Geología de sus pegmatitas. Rev Asoc Geol Arg. 1983;38:340-80.
George, L., Cook, N.J., Ciobanu, C.L., Wade, B.P., 2015. Trace and minor elements in galena: A reconnaissance LA-ICP-MS study. American Mineralogist. 100, 548–569.
George, L.L., Cook, N.J., Ciobanu, C.L., 2016. Partitioning of trace elements in co-crystallized sphalerite–galena–chalcopyrite hydrothermal ores. Ore Geology Reviews. 77, 97–116.
George, L.L., Cook, N.J., Ciobanu, C.L., 2017. Minor and trace elements in natural tetrahedrite-tennantite: Effects on element partitioning among base metal sulphides. Minerals. 7, 17.
George, L.L., Cook, N.J., Crowe, B.B., Ciobanu, C.L., 2018. Trace elements in hydrothermal chalcopyrite. Mineralogical Magazine. 82, 59–88.
Giuliani, G., Li, Y., Sheng, T., 1988. Fluid inclusion study of Xihuashan tungsten deposit in the southern Jiangxi province. China. Mineralium Deposita. 23, 24–33.
Gołębiowska, B., Pieczka, A., Parafiniuk, J., 2012. Substitution of Bi for Sb and As in minerals of the tetrahedrite series from Rędziny, Lower Silesia, southwestern Poland. The Canadian Mineralogist. 50, 267–279.
Gorse-Pomonti, D., Russier, V., 2007. Liquid metals for nuclear applications. Journal of Non-Crystalline Solids. 353, 3600–3614.
Graedel, T., Allwood, J., Birat, J., Reck, B., Sibley, S., Sonnemann, G., et al., 2011. Recycling Rates of Metals, A Status Report. A Report of the Working Group on the Global Metal Flows to the International Resource Panel. United Nations Environment Programme.
Graeser, S., 1969. Minor elements in sphalerite and galena from Binnatal. Contributions to Mineralogy and Petrology. 24, 156–163.
Grant, H.L., Layton-Matthews, D., Peter, J.M., 2015. Distribution and controls on silver mineralization in the Hackett River Main Zone, Nunavut, Canada: An Ag-and Pb-enriched archean volcanogenic massive sulfide deposit. Economic Geology. 110, 943–982.
Grant, J.N.M., 1979. A study of ore genesis and geochronology in the sub-volcanic tin belt of the Eastern Andes. Imperial College London, Bolivia.
Greenland, L., Gottfried, D., Campbell, E., 1973. Aspects of the magmatic geochemistry of bismuth. Geochimica et Cosmochimica Acta. 37, 283–295.
Groznova, E.O., Dobrovol'skaya, M.G., Kovalenker, V.A., Tsepin, A.I., Razin, M.V., 2005. Bismuth mineralisation of Pb Zn ores at the Djimidon deposit (North Osetia). New Data on Minerals. 72.
Guimarães, F.S., Cabral, A.R., Lehmann, B., Rios, F.J., Ávila, M.A.B., de Castro, M.P., et al., 2019. Bismuth-melt trails trapped in cassiterite–quartz veins. Terra Nova.
Gvozdev, V., 2009. Bismuth mineralization in ores of the Skrytoe scheelite deposit (Primorye) and problems of its genesis. Russian Journal of Pacific Geology. 3, 69.
Ha, T.K., Kwon, B.H., Park, K.S., Mohapatra, D., 2015. Selective leaching and recovery of bismuth as Bi_2O_3 from copper smelter converter dust. Separation and Purification Technology. 142, 116–122.
Hale, M., 1981. Pathfinder applications of arsenic, antimony and bismuth in geochemical exploration. Developments in Economic Geology: Elsevier 307–323.
Hart, C.J., 2005. Classifying, distinguishing and exploring for intrusion-related gold systems. The Gangue. 87, 4–9.
Hart CJ. Reduced intrusion-related gold systems. In: Goodfellow W, editor. Mineral deposits of Canada: A Synthesis of Major Deposit Types, District Metallogeny, the Evolution of Geological Provinces, and Exploration Methods: Geological Association of Canada, Mineral Deposits Division, Special Publication No. 5; 2007. p. 95-112.
Hart CJ, Baker T, Burke M. New exploration concepts for country-rock-hosted, intrusion-related gold systems: Tintina gold belt in Yukon. In: TL Tucker, MT Smith, editors. The Tintina gold belt: concepts, exploration and discoveries British Columbia and Yukon Chamber of Mines, Special Volume 2000. p. 145-72.
Hau, N.T., Nevolko, P., Dung, P.T., Svetlitskaya, T., Hoa, T.T., Shelepaev, R., et al., 2020. Age and genesis of the W-Bi-Cu-F (Au) Nui Phao deposit, Northeast Vietnam: Constrains from U-Pb and Ar-Ar geochronology, fluid inclusions study, S-O isotope systematic and scheelite geochemistry. Ore Geology Reviews. 103578.
Henry, D., Birch, W., 2022. The Wombat Hole Prospect, Benambra, Victoria, Australia: A Cu–Bi–(Te) exoskarn with unusual supergene mineralogy. Mineralogical Magazine 1–39. https://doi.org/10.1180/mgm.2022.11. In press.
Hey, M.H., 1938. Russellite, a new British mineral. Mineralogical Magazine. 25, 41–55.
Hood, S.B., Cracknell, M.J., Gazley, M.F., Reading, A.M., 2019. Element mobility and spatial zonation associated with the Archean Hamlet orogenic Au deposit, Western Australia: Implications for fluid pathways in shear zones. Chemical Geology. 514, 10–26.
Ishihara, S., Orihashi, Y., 2014. Zircon U-Pb age of the Triassic granitoids at Nui Phao, northern Viet Nam. Bulletin of the Geological Survey of Japan. 65, 17–22.
Jain, S.M., Edvinsson, T., Durrant, J.R., 2019. Green fabrication of stable lead-free bismuth based perovskite solar cells using a non-toxic solvent. Communications Chemistry. 2, 1–7.
JEITA. Representative Organizations from Japan, United States and Europe Begin Preparing the World Lead-free Soldering Roadmap and Agree to Eliminate Lead by 2005. 2002.
Jenkin, G.R., Al-Bassam, A.Z., Harris, R.C., Abbott, A.P., Smith, D.J., Holwell, D.A., et al., 2016. The application of deep eutectic solvent ionic liquids for environmentally-friendly dissolution and recovery of precious metals. Minerals Engineering. 87, 18–24.
Jenner, F.E., 2017. Cumulate causes for the low contents of sulfide-loving elements in the continental crust. Nature Geoscience. 10, 524–529.
Jochum, K., Hofmann, A., 1997. Constraints on earth evolution from antimony in mantle-derived rocks. Chemical geology. 139, 39–49.
John, D.A., Taylor, R.D., 2016. By-Products of Porphyry Copper and Molybdenum Deposits. In: Verplanck, P.L., Hitzman, M.W. (Eds.), Rare Earth and Critical Elements in Ore Deposits: Society of Economic Geologists.
Johnson, N.E., Craig, J.R., Rimstidt, J.D., 1986. Compositional trends in tetrahedrite. The Canadian Mineralogist. 24, 385–397.
Kasatkin, A.V., Makovicky, E., Plášil, J., Škoda, R., Agakhanov, A.A., Stepanov, S.Y., et al., 2020. Luboržákite, Mn_2AsSbS_5, a new member of pavonite homologous series from Vorontsovskoe gold deposit, Northern Urals. Russia. Mineralogical Magazine. 84, 738–745.
Keim, M.F., Staude, S., Marquardt, K., Bachmann, K., Opitz, J., Markl, G., 2018. Weathering of Bi-bearing tennantite. Chemical Geology.
Keith, M., Häckel, F., Haase, K.M., Schwarz-Schampera, U., Klemd, R., 2016. Trace element systematics of pyrite from submarine hydrothermal vents. Ore Geology Reviews. 72, 728–745.
Kettaneh, Y., Badham, J., 1978. Mineralization and paragenesis at the Mount Wellington Mine. Cornwall. Economic Geology. 73, 486–495.
KGHM Polska Miedź S.A. Analyst Day Presentation. 2019.
Kim, T.W., Ping, Y., Galli, G.A., Choi, K.-S., 2015. Simultaneous enhancements in photon absorption and charge transport of bismuth vanadate photoanodes for solar water splitting. Nature communications. 6, 1–10.
Kissin SA. Five-element (Ni-Co-As-Ag-Bi) veins. Geoscience Canada. 1992;19.
Knights KV. Tellus geochemical survey: deeper topsoil data from outer Dublin the border, north, and west of Ireland Geological Survey of Ireland; 2020.
Koděra, M., Kupčík, V., Makovický, E., 1970. Hodrushite—A new sulphosalt. Mineralogical Magazine. 37, 641–648.
Kolonin, G., Laptev, Y.V., 1982. Study of process of dissolution of alpha-Bi_2O_3 (bismite) and complex-formation of bismuth in hydrothermal systems. Geokhimiya. 1621–31.
Kooiman, G., McLeod, M., Sinclair, W., 1986. Porphyry tungsten-molybdenum orebodies, polymetallic veins and replacement bodies, and tin-bearing greisen zones in the Fire Tower Zone, Mount Pleasant. New Brunswick. Economic Geology. 81, 1356–1373.
Koski, R.A., Benninger, L.M., Zierenberg, R.A., Jonasson, I.R., 1994. Composition and growth history of hydrothermal deposits in Escanaba Trough, southern Gorda Ridge. US Geological Survey Bulletin. 2022, 293–324.
Koski, R.A., Shanks III, W.C., Bohrson, W.A., Oscarson, R.L., 1988. Composition of massive sulfide deposits from the sediment-covered floor of Escanaba Trough, Gorda Ridge: implications for depositional processes. Canadian Mineralogist 655–673.
Kotlyar BB, Ludington S, Mosier DL. Descriptive, Grade, and Tonnage Models for Molybdeum-Tungsten Greisen Deposits Open-File Report 95-584 U.S. Geological Survey; 1995.
Krenev, V., Drobot, N., Fomichev, S., 2015. Processes for the recovery of bismuth from ores and concentrates. Theoretical Foundations of Chemical Engineering. 49, 540–544.
Kruszewski, J.M., Wood, S.A., 2009. Experimental measurement of the solubility of bismuth phases in water vapor from 220° C to 300° C: Implications for ore formation. Applied geochemistry. 24, 493–503.
Kyle J, Breuer P, Bunney K, Pleysier R, May P. Review of trace toxic elements (Pb, Cd, Hg, As, Sb, Bi, Se, Te) and their deportment in gold processing. Part 1: Mineralogy, aqueous chemistry and toxicity. Hydrometallurgy. 2011;107:91-100.
Lacinska, A., Rochelle, C., 2019. Petrographic description of selected samples from the exhumed geothermal system at Las Minas, Trans-Mexican Volcanic Belt. Open Report OR/19/007. British Geological Survey.
Lambert, J.R., 1991. Pharmacology of bismuth-containing compounds. Reviews of infectious diseases. 13, S691–S695.
Large, R., 1974. Gold-bismuth-copper mineralisation in the Tennant Creek district, Northern Territory. University of Tasmania, Australia.
Lawrence, D.M., Treloar, P.J., Rankin, A.H., Harbidge, P., Holliday, J., 2013. The geology and mineralogy of the Loulo mining district, Mali, West Africa: Evidence for two distinct styles of orogenic gold mineralization. Economic Geology. 108, 199–227.
Li, W., Cook, N.J., Ciobanu, C.L., Xie, G., Wade, B.P., Gilbert, S.E., 2019. Trace element distributions in (Cu)-Pb-Sb sulfosalts from the Gutaishan Au-Sb deposit, South China: Implications for formation of high fineness native gold. American Mineralogist: Journal of Earth and Planetary Materials. 104, 425–437.
Lin, J.-C., Sharma, R., Chang, Y., 1996. The Bi-S (bismuth-sulfur) system. Journal of Phase Equilibria. 17, 132–139.
Lipinski, M., Warning, B., Brumsack, H.-J., 2003. Trace metal signatures of Jurassic/Cretaceous black shales from the Norwegian Shelf and the Barents Sea. Palaeogeography, Palaeoclimatology, Palaeoecology. 190, 459–475.
Long, K., Ludington, S., Du Bray, E., Andre-Ramos, O., McKee, E., 1992. Geology and mineral deposits of the La Joya district, Bolivia. SEG Newsletter. 10.
Lu, H.-Z., Liu, Y., Wang, C., Xu, Y., Li, H., 2003. Mineralization and fluid inclusion study of the Shizhuyuan W-Sn-Bi-Mo-F skarn deposit, Hunan Province. China. Economic Geology. 98, 955–974.

Makovicky, E., Mumme, W., Watts, J., 1977. The crystal structure of synthetic pavonite, AgBi3S5, and the definition of the pavonite homologous series. The Canadian Mineralogist. 15, 339–348.
Makovicky, E., Topa, D., 2014. Lillianites and andorites: new life for the oldest homologous series of sulfosalts. Mineralogical Magazine. 78, 387–414.
Mao, J., Guy, B., Raimbault, L., Shimazaki, H., 1996. Manganese skarn in the Shizhuyuan polymetallic tungsten deposit, Hunan. China. Shigen-Chishitsu. 46, 1–11.
Marcoux, E., Moëlo, Y., Leistel, J., 1996. Bismuth and cobalt minerals as indicators of stringer zones to massive sulphide deposits. Iberian Pyrite Belt. Mineralium Deposita. 31, 1–26.
Mariko, T., Kawada, M., Miura, M., Ono, S., 1996. Ore Formation Processes of The Mozumi Skarn-type Pb-Zn-Ag Deposit in the Kamioka Mine, Gifu Prefecture. Central Japan. Shigen-Chishitsu. 46, 337–354.
Markl G. Schwarzwald: Bode; 2015.
Markl, G., Burisch, M., Neumann, U., 2016. Natural fracking and the genesis of five-element veins. Mineralium Deposita. 51, 703–712.
Markowski, A., Vallance, J., Chiaradia, M., Fontboté, L., 2006. Mineral zoning and gold occurrence in the Fortuna skarn mine, Nambija district. Ecuador. Mineralium Deposita. 41, 301–321.
Márquez-Zavalía, M.F., Galliski, M.Á., Černý, P., Chapman, R., 2012. An assemblage of bismuth-rich, tellurium-bearing minerals in the El Quemado granitic pegmatite, Nevados de Palermo, Salta. Argentina. The Canadian Mineralogist. 50, 1489–1498.
Martin, A.J., Keith, M., McDonald, I., Haase, K.M., McFall, K.A., Klemd, R., et al., 2019. Trace element systematics and ore-forming processes in mafic VMS deposits: Evidence from the Troodos ophiolite. Cyprus. Ore Geology Reviews. 106, 205–225.
Masan Resources. 2013 Sustainability report [online]. 2014a.
Masan Resources. Resources and Reserves estimate [online]. 2014b.
Masan Resources. Nui Phao Geology. 2016.
Masan Resources. Annual and Sustainability Report 2020. 2020.
Maslennikov, V., Maslennikova, S., Large, R., Danyushevsky, L., Herrington, R., Ayupova, N., et al., 2017. Chimneys in Paleozoic massive sulfide mounds of the Urals VMS deposits: Mineral and trace element comparison with modern black, grey, white and clear smokers. Ore Geology Reviews. 85, 64–106.
Matsukuma, T., 1961. Gold and silver deposits and their ores in Kyushu, Japan, Part I. Journal of the Mining College, Akita University: Mining geology Series A. 1, 20.
Mazurov A. The Koktenkol stockwork W-Mo deposit, central Kazakhstan. Granite-Related Ore Deposits of Central Kazakhstan and Adjacent Areas 1996. p. 155-65.
McCoy, D., 1997. Plutonic-related gold deposits of interior Alaska. Mineral Deposits of Alaska Econ Geol Monogr. 9, 191–241.
McCoy, D.T., 2000. Mid-Cretaceous plutonic-related gold deposits of interior Alaska: Metallogenesis, characteristics, gold-associative mineralogy and geochronology. University of Alaska Fairbanks.
McDonough, W.F., Sun, S.-S., 1995. The composition of the Earth. Chemical geology. 120, 223–253.
Meinert, L., 2000. Gold in skarns related to epizonal intrusions. Reviews in Economic Geology. 13, 347–375.
Meinert, L.D., 1992. Skarns and skarn deposits. Geoscience Canada. 19.
Micon International Ltd. Technical report on the feasibility study for the NICO gold-cobalt-bismuth-copper project, Northwest Territories, Canada [online]. 2014.
Mintser, E., 1979. The geochemical properties of the behavior of bismuth in hypogenic processes. Geochemistry of Bismuth: Benchmark Papers in Geology: Stroudsburg, Pennsylvania, Dowden, Hutchinson and Ross. 49, 268–327.
Mohan, R., 2010. Green bismuth. Nature chemistry. 2, 336.
Moles, N.R., Tindle, A.G., 2012. Tungsten and bismuth minerals, including russellite, within greisen veins in the western Mourne Mountains, Northern Ireland. Journal of the Russell Society. 15, 40–48.
Monecke, T., Petersen, S., Hannington, M.D., Grant, H., Samson, I., 2016. The minor element endowment of modern sea-floor massive sulfide deposits and comparison with deposits hosted in ancient volcanic successions. In: Verplanck, P.L., Hitzman, M.W. (Eds.), Rare Earth and Critical Elements in Ore Deposits: Society of Economic Geologists.
Mosier, D.L., Singer, D., Salem, B., 1983. Geologic and grade-tonnage information on volcanic-hosted copper-zinc-lead massive sulfide deposits. US Geological Survey.
Mustard, R., 2001. Granite-hosted gold mineralization at Timbarra, northern New South Wales. Australia. Mineralium Deposita. 36, 542–562.
Mustard, R., Ulrich, T., Kamenetsky, V.S., Mernagh, T., 2006. Gold and metal enrichment in natural granitic melts during fractional crystallization. Geology. 34, 85–88.
Naumov, G., Vlasov, B., Golubev, V., Mironova, O., 2017. The Schlema-Alberoda five-element uranium deposit, Germany: An example of self-organizing hydrothermal system. Geology of Ore Deposits. 59, 1–13.
Nörtemann M. Geological mapping of the Goldkuppe area on the farms Otjimbojo and Otjakatjongo in the central Damara-Orogen, Namibia, & Genesis, Petrography and Mineral Chemistry of the Goldskarn deposit Navachab in the central Damara-Orogen, Namibia. Unpubl: Diploma thesis, University of Göttingen, Germany; 1997.
Nörtemann, M.-F.-J., Mücke, A., Weber, K., Meinert, L.D., 2000. Mineralogy of the Navachab skarn deposit, Namibia: an unusual Au-bearing skarn in high-grade metamorphic rocks. Communications of the Geological Survey of Namibia. 12, 149–156.
Oberthür, T., Weiser, T., 2008. Gold-bismuth-telluride-sulphide assemblages at the Viceroy Mine, Harare-Bindura-Shamva greenstone belt. Zimbabwe. Mineralogical Magazine. 72, 953–970.
Oelsner, O., 1958. Die erzgebirgischen Granite, ihre Vererzung und die Stellung der Bi-Co-Ni-Formation innerhalb der Vererzung. Geologie. 7, 682–697.
Oen, I., Kieft, C., 1976. Silver-bearing wittichenite-chalcopyrite-bornite intergrowths and associated minerals in the Mangualde pegmatite. Portugal. The Canadian Mineralogist. 14, 185–193.
Oen, I., Kieft, C., 1984. Paragenetic relations of Bi-, Ag-, Au-, and other tellurides in bornite veins at Glava, Värmland. Sweden. Neues Jahrbuch für Mineralogie Abhandlungen. 149, 245–266.
Ondrus, P., Veselovsky, F., Gabasova, A., Drabek, M., Dobes, P., Hlousek, J., et al., 2003. Ore-forming processes and mineral parageneses of the Jáchymov ore district. Journal of GEOsciences. 48, 157–192.
Otto, A., Dziggel, A., Kisters, A., Meyer, F., 2007. The New Consort Gold Mine, Barberton greenstone belt, South Africa: orogenic gold mineralization in a condensed metamorphic profile. Mineralium Deposita. 42, 715–735.
Parrish, I., Tully, J., 1978. Porphyry tungsten zones at Mt Pleasant. New Brunswick. CIM Bull. 71, 93–100.
Petříček, V., Makovicky, E., 2006. Interpretation of selected structures of the bismuthinite–aikinite series as commensurately modulated structures. The Canadian Mineralogist. 44, 189–206.
Phillips, G.N., Powell, R., 2015. A practical classification of gold deposits, with a theoretical basis. Ore Geology Reviews. 65, 568–573.
Piestrzyński, A., Wendorff, M., Letsholo, M., Mackay, W., 2015. Platinum-group minerals in the Neoproterozoic stratabound copper-silver mineralisation, the Kalahari Copperbelt, northwestern Botswana. South African Journal of Geology. 118, 275–284.
Plotinskaya, O.Y., Kovalenker, V., Seltmann, R., Stanley, C., 2006. Te and Se mineralogy of the high-sulfidation Kochbulak and Kairagach epithermal gold telluride deposits (Kurama Ridge, Middle Tien Shan, Uzbekistan). Mineralogy and Petrology. 87, 187–207.
Polya, D., 1989. Chemistry of the main-stage ore-forming fluids of the Panasqueira W-Cu (Ag)-Sn deposit, Portugal; implications for models of ore genesis. Economic Geology. 84, 1134–1152.
Pring, A., Etschmann, B., 2002. Crystal chemistry of cosalite, and its relationship to the lillianite group. Mineral Mag. 66, 451–458.
Rayment, B., Davis, G., Willson, J., 1971. Controls to mineralization at Wheal Jane, Cornwall. Transactions of the Institution of Mining and Metallurgy, London. 80, 224B–237B.
Reimann C, Birke M, Demetriades A, Filzmoser P, O'Connor P. Chemistry of Europe's agricultural soils, part A. 2014.
Renner, S., Wellmer, F.W., 2019. Volatility drivers on the metal market and exposure of producing countries. Mineral. Economics. 1–30.
Richards, J., Dang, T., Dudka, S., Wong, M., 2003. The Nui Phao tungsten-fluorite-copper-gold-bismuth deposit, northern Vietnam: An opportunity for sustainable development. Exploration and Mining Geology. 12, 61–70.
Rudnick, R.L., Gao, S., 2003. Composition of the continental crust. Treatise on geochemistry. 3, 659.
Rundquist, D., 1982. Zoning of metallization associated with acid magmatism. Metallization Associated with Acid Magmatism. 6, 279–289.
Sahama, T.G., Lehtinen, M., 1968. Bismutite of the granite pegmatites of Zambezia, Mozambique. Bulletin of the Geological Society of Finland. 40, 145–150.
Sanematsu, K., Ishihara, S., 2011. $^{40}Ar/^{39}Ar$ ages of the Da Lien granite related to the Nui Phao W mineralization in northern Vietnam. Resource geology. 61, 304–310.
Satterthwaite, C., Ure Jr, R., 1957. Electrical and thermal properties of Bi_2Te_3. Physical Review. 108, 1164.
Seccombe P, Downes P, Ashley P, BrathwaiteE R, Green G, Murray C, et al. World Skarn Deposits: Skarn Deposits of the Southwest Pacific. In: Hedenquist JW, Thompson JFH, Goldfarb RJ, P.Richards J, editors. Economic Geology 100th Anniversary Volume Society of Economic Geologists, Littleton, Colorado, USA; 2005. p. 299-336.
Selby, D., Nesbitt, B.E., Muehlenbachs, K., Prochaska, W., 2000. Hydrothermal Alteration and Fluid Chemistry of the Endako Porphyry Molybdenum Deposit. British Columbia. Economic Geology. 95, 183–202.
Seltmann, R., Štemprok, M., 1994. Textural evidence for the existence of two-phase granites in the Younger Intrusive Complex granites of the Krušné Hory/Erzgebirge province. J Czech Geol Soc. 39, 103–104.
Sharpe, J.L., Williams, P.A., 2004. Secondary bismuth and molybdenum minerals from Kingsgate, New England district of New South Wales. Australian Journal of Mineralogy.
Simanenko, L., 2007. Modes of trace element occurrence in galena from the Partizansky base metal-skarn deposit. Primorye. Russian Journal of Pacific Geology. 1, 144–152.
Simons, B., Andersen, J.C., Shail, R.K., Jenner, F.E., 2017. Fractionation of Li, Be, Ga, Nb, Ta, In, Sn, Sb, W and Bi in the peraluminous Early Permian Variscan granites of the Cornubian Batholith: precursor processes to magmatic-hydrothermal mineralisation. Lithos. 278, 491–512.
Skirrow, R.G., 2000. Gold-copper-bismuth deposits of the Tennant Creek district, Australia: A reappraisal of diverse high-grade systems. Hydrothermal Iron Oxide Copper-Gold and Related Deposits: Adelaide, Australian Mineral Foundation. 1, 149–160.
Skirrow, R.G., Huston, D.L., Mernagh, T.P., Thorne, J.P., Duffer, H., Senior, A., 2013. Critical commodities for a high-tech world: Australia's potential to supply global demand. Geoscience Australia Canberra.
Skirrow, R.G., Walshe, J.L., 2002. Reduced and oxidized Au-Cu-Bi iron oxide deposits of the Tennant Creek Inlier, Australia: An integrated geologic and chemical model. Economic Geology. 97, 1167–1202.
Škoda, R., Novák, M., Čopjaková, R., Galliski, M.Á., Márquez-Zavalía, M.F., Sejkora, J., 2021. Bismuth Minerals from the Intragranitic La Elsa NYF Pegmatite, Potrerillos Granite, Argentina: Monitors of Fluid Evolution from Magmatic to Hydrothermal Stage. The Canadian Mineralogist.
Slikkerveer, A., de Wolff, F.A., 1989. Pharmacokinetics and toxicity of bismuth compounds. Medical toxicology and adverse drug experience. 4, 303–323.
Smith J. Arsenic, antimony and bismuth. Comprehensive inorganic chemistry: Elsevier. 1973. 547-683.

Smith, R.E., Perdrix, J., 1983. Pisolitic laterite geochemistry in the Golden Grove massive sulphide district, Western Australia. Journal of Geochemical Exploration. 18, 131–164.
Sobolev, V., Benamati, G., 2007. Thermophysical and electric properties. Materials Compatibility, Thermal-hydraulics and Technologies, Handbook on Lead-bismuth Eutectic Alloy and Lead Properties, pp. 25–99.
Staude, S., Mordhorst, T., Neumann, R., Prebeck, W., Markl, G., 2010. Compositional variation of the tennantite–tetrahedrite solidsolution series in the Schwarzwald ore district (SW Germany): the role of mineralization processes and fluid source. Mineralogical Magazine. 74, 309–339.
Staude, S., Werner, W., Mordhorst, T., Wemmer, K., Jacob, D.E., Markl, G., 2012. Multi-stage Ag–Bi–Co–Ni–U and Cu–Bi vein mineralization at Wittichen, Schwarzwald, SW Germany: geological setting, ore mineralogy, and fluid evolution. Mineralium Deposita. 47, 251–276.
Štemprok, M., 1995. A comparison of the Krušné Hory-Erzgebirge (Czech Republic–Germany) and Cornish (UK) granites and their related mineralizations. In: Proceedings of the Ussher Society, pp. 347–356.
Štemprok, M., Pivec, E., Langrová, A., 2005. The petrogenesis of a wolframite-bearing greisen in the Vykmanov granite stock, Western Krušné hory pluton (Czech Republic). Bulletin of Geosciences. 80, 163–184.
Sugaki, A., Kitakaze, A., Hayashi, K., 1981. Synthesis of minerals in the Cu-Fe-Bi-S system under hydrothermal condition and their phase relations. Bulletin de Mineralogie. 104, 484–495.
Sugaki, A., Kojima, S., Shimada, N., 1988. Fluid inclusion studies of the polymetallic hydrothermal ore deposits in Bolivia. Mineralium Deposita. 23, 9–15.
Suksongkarm, P., Rojananan, S., Rojananan, S., 2017. Using recycled bismuth-tin solder in novel machinable lead-free brass. Materials Transactions. M2017227.
Tarafder, A., Singh, S.P., Karmakar, B., 2010. Environmentally Friendly and New Generation Glasses for Plasma TV. Kanch. 4, 42–48.
Terlain, A., Sobolev, V., Courouau, J.-L., Martinelli, L., Agostini, P., Ciampichetti, A., et al., 2007. Chapter 3: thermodynamic relationships and heavy liquid metal interaction with other coolants. In: Fazio, C. (Ed.), Handbook on Lead–bismuth Eutectic Alloy and Lead Properties, Materials Compatibility, Thermal-hydraulics and Technologies. Nuclear Energy Agency, Paris.
Testa, F.J., Cooke, D.R., Zhang, L., Mas, G.R., 2016;6:62.. Bismoclite (BiOCl) in the San Francisco de los Andes Bi–Cu–Au Deposit, Argentina. First Occurrence of a Bismuth Oxychloride in a Magmatic-Hydrothermal Breccia Pipe and Its Usefulness as an Indicator Phase in Mineral Exploration. Minerals.
Testa, F.J., Zhang, L., Cooke, D.R., 2018. Physicochemical conditions of formation for bismuth mineralization hosted in a magmatic-hydrothermal breccia complex: an example from the Argentine Andes. Minerals. 8, 486.
Theodore TG, Orris GJ, Hammerstrom JM, Bliss JD. Gold-bearing skarns. USGPO; 1991.
Thompson, J., Sillitoe, R., Baker, T., Lang, J., Mortensen, J., 1999. Intrusion-related gold deposits associated with tungsten-tin provinces. Mineralium Deposita. 34, 323–334.
Tomkins, A.G., Pattison, D.R., Frost, B.R., 2007. On the initiation of metamorphic sulfide anatexis. Journal of Petrology. 48, 511–535.
Tooth, B., Brugger, J., Ciobanu, C., Liu, W., 2008. Modeling of gold scavenging by bismuth melts coexisting with hydrothermal fluids. Geology. 36, 815–818.
Tooth, B., Ciobanu, C.L., Green, L., O'Neill, B., Brugger, J., 2011. Bi-melt formation and gold scavenging from hydrothermal fluids: An experimental study. Geochimica et Cosmochimica Acta. 75, 5423–5443.
Tooth, B., Etschmann, B., Pokrovski, G.S., Testemale, D., Hazemann, J.-L., Grundler, P. V., et al., 2013. Bismuth speciation in hydrothermal fluids: An X-ray absorption spectroscopy and solubility study. Geochimica et Cosmochimica Acta. 101, 156–172.
Topa, D., Makovicky, E., Paar, W.H., 2002. Composition ranges and exsolution pairs for the members of the bismuthinite–aikinite series from Felbertal. Austria. The Canadian Mineralogist. 40, 849–869.
Törmänen, T.O., Koski, R.A., 2005. Gold enrichment and the Bi-Au association in pyrrhotite-rich massive sulfide deposits, Escanaba Trough. Southern Gorda Ridge. Economic Geology. 100, 1135–1150.
U.S. Department of the Interior, 2018. Final List of Critical Minerals 2018, 23295–23296.
U.S. Geological Survey, 1994. Bismuth. Minerals Yearbook.
U.S. Geological Survey, 1996. Bismuth. Minerals Yearbook.
U.S. Geological Survey, 2013. Bismuth. Mineral Commodity Summaries.
U.S. Geological Survey. 2015 Minerals Yearbook; Bismuth. Minerals Yearbook 2017.
U.S. Geological Survey, 2018. Bismuth. Mineral Commodity Summaries.
U.S. Geological Survey, 2020. Bismuth Mineral Commodity Summaries.
U.S. Geological Survey, 2021. Bismuth. Mineral Commodity Summaries.
Ulrich, G.H., 1869. Observations on the "Nuggetty Reef', Mount-Tarrangower Gold-Field. Quarterly Journal of the Geological Society. 25, 326–335.
UN Economic and Social Council. Case studies and testing of the United Nations Framework Classification for Fossil Energy and Mineral Reserves and Resources 2009 In: Economic Commission for Europe Committee on Sustainable Energy, editor.2014. p. 32.
Völz, H.G., Kischkewitz, J., Woditsch, P., Westerhaus, A., Griebler, W.D., De Liedekerke, M., et al., 2006. Pigments, inorganic. Ullmann's Encyclopedia of Industrial. Chemistry.
von Knorring, O., Fadipe, A., 1981. On the mineralogy and geochemistry of niobium and tantalum in some granite pegmatites and alkali granites of Africa. Bulletin de Minéralogie. 104, 496–507.
Voronin, M.V., Osadchii, E.G., 2013. Thermodynamic properties of silver and bismuth sulfosalt minerals, pavonite ($AgBi_3S_5$) and matildite ($AgBiS_2$) and implications for ore deposits. Economic Geology. 108, 1203–1210.
Voudouris, P.C., Spry, P.G., Mavrogonatos, C., Sakellaris, G.-A., Bristol, S.K., Melfos, V., et al., 2013. Bismuthinite derivatives, lillianite homologues, and bismuth sulfotellurides as indicators of gold mineralization in the Stanos shear-zone related deposit, Chalkidiki. Northern Greece. The Canadian Mineralogist. 51, 119–142.
Wagner, T., 2007. Thermodynamic modeling of Au-Bi-Te melt precipitation from high-temperature hydrothermal fluids: Preliminary results. The Ninth Biennial SGA Meeting. Dublin 769–772.
Wang, N., 1999. An experimental study of some solid solutions in the system Ag_2S-PbS-Bi_2S_3 at low temperatures. J Neues Jahrbuch für Mineralogie Monatshefte. 223–240.
Wang, R., Lai, T.-P., Gao, P., Zhang, H., Ho, P.-L., Woo, P.-C.-Y., et al., 2018. Bismuth antimicrobial drugs serve as broad-spectrum metallo-β-lactamase inhibitors. Nature communications. 9, 1–12.
Wasserstein, B., 1951. Precision lattice measurements of galena. American Mineralogist: Journal of Earth and Planetary Materials. 36, 102–115.
Wimmers, D., 1985. Silver minerals of Panasqueira, Portugal: a new occurrence of Te-bearing canfieldite. Mineralogical Magazine. 49, 745–748.
Wu, F.-Y., Liu, X.-C., Liu, Z.-C., Wang, R.-C., Xie, L., Wang, J.-M., et al., 2020. Highly fractionated Himalayan leucogranites and associated rare-metal mineralization. Lithos. 352, 105319.
Wu, S., Chen, R., Zhang, S., Babu, B.H., Yue, Y., Zhu, H., et al., 2019. A chemically inert bismuth interlayer enhances long-term stability of inverted perovskite solar cells. Nature communications. 10, 1–11.
Wu, S., Mao, J., Yuan, S., Dai, P., Wang, X., 2018. Mineralogy, fluid inclusion petrography, and stable isotope geochemistry of Pb–Zn–Ag veins at the Shizhuyuan deposit, Hunan Province, southeastern China. Mineralium Deposita. 53, 89–103.
Xilin, L., 1990. Bismuthoan galena—A new variety of galena. Chinese Journal of Geochemistry. 9, 378–384.
Zaw, K., Huston, D., Large, R., Mernagh, T., Hoffmann, C., 1994. Microthermometry and geochemistry of fluid inclusions from the Tennant Creek gold-copper deposits: Implications for ore deposition and exploration. Mineralium Deposita. 29, 288–300.
Zhang, L., Wen, H., Qin, C., Du, S., Zhu, C., Fan, H., et al., 2015. The geological significance of Pb–Bi-and Pb–Sb-sulphosalts in the Damajianshan tungsten polymetallic deposit, Yunnan Province. China. Ore Geology Reviews. 71, 203–214.
Zhong, J., Chen, Y.-J., Pirajno, F., 2017. Geology, geochemistry and tectonic settings of the molybdenum deposits in South China: A review. Ore Geology Reviews. 81, 829–855.
Zhou, H., Sun, X., Cook, N.J., Lin, H., Fu, Y., Zhong, R., et al., 2017. Nano-to micron-scale particulate gold hosted by magnetite: A product of gold scavenging by bismuth melts. Economic Geology. 112, 993–1010.
Zhou, H., Sun, X., Fu, Y., Lin, H., Jiang, L., 2016. Mineralogy and mineral chemistry of Bi-minerals: Constraints on ore genesis of the Beiya giant porphyry-skarn gold deposit, southwestern China. Ore Geology Reviews. 79, 408–424.
Zhou, H., Wirth, R., Gleeson, S.A., Schreiber, A., Mayanna, S., 2021. Three-dimensional and microstructural fingerprinting of gold nanoparticles at fluid-mineral interfaces. American Mineralogist: Journal of Earth Planetary Materials. 106, 97–104.
Zierenberg, R.A., Koski, R.A., Morton, J.L., Bouse, R.M., 1993. Genesis of massive sulfide deposits on a sediment-covered spreading center, Escanaba Trough, southern Gorda Ridge. Economic Geology. 88, 2069–2098.